

## ANALYSIS

[View Article Online](#)  
[View Journal](#) | [View Issue](#)

Cite this: *Energy Environ. Sci.*, 2023, 16, 1821

## Emerging concepts in intermediate carbon dioxide emplacement to support carbon dioxide removal†

Hanna Marie Breunig, \* Fabian Rosner, Tae-Hwan Lim and Peng Peng

Substantial upscaling of carbon dioxide capture is possible in the coming decades but existing solutions for storage are projected to be limited in annual capacity by as much as 2–10 GtCO<sub>2</sub> per year until mid-century. Temporary storage of CO<sub>2</sub> in a solid or liquid state could prove useful for filling this gap in capacity, until more permanent and ideally lucrative CO<sub>2</sub> sequestration options come online. There are several concepts for reversible solid-state and chemical CO<sub>2</sub> storage, but their advantages and limitations have yet to be reviewed in this context. This article focuses on the physical and chemical aspects of CO<sub>2</sub> storage via liquid and solid chemical carriers and sorbents, and gives an overview of the energetics around their use, as well as prospects for their future development. Exciting opportunities for coupling capture and medium to high maturity multi-year storage technologies could support carbon removal in the coming decades. Highlights of the analysis are the remarkable storage capacity of oxalic acid and formic acid (CO<sub>2</sub>-density of 1857 kg m<sup>-3</sup> and 1152 kg m<sup>-3</sup>, compared with condensed liquid CO<sub>2</sub> at 993–1096 kg m<sup>-3</sup>, respectively), the relative scalability and compatibility of carbonate salts for stationary storage with direct air capture, and the potential promise of multiple carriers for CO<sub>2</sub> transportation. Solid sorbents do not achieve such ultra-high storage capacities, but could improve storage over compressed gas tanks on a capacity and energetics basis.

Received 8th November 2022,  
Accepted 27th March 2023

DOI: 10.1039/d2ee03623a

rsc.li/ees

## Broader context

To mitigate climate change, we must move an enormous amount of CO<sub>2</sub> out of the atmosphere, greater than any mass moved by humanity to date (~473 Gt to lower CO<sub>2</sub> concentration to 350 ppm). Identifying CO<sub>2</sub> storage solutions to serve booming CO<sub>2</sub> capture developments until permanent geologic storage options come online remains an underappreciated scientific challenge of the highest importance.

## Introduction

Carbon dioxide removal (CDR) technologies can slow the accumulation of CO<sub>2</sub> in the atmosphere if deployed in the first half of the century, which is essential for staying below 2 °C warming.<sup>1</sup> Direct air capture (DAC) and bioenergy with carbon capture and sequestration (BECCS) are commercially viable CDR technologies that generate gas with high concentrations of CO<sub>2</sub>. Cost predictions from the IPCC and some of this study's authors suggest that deploying these and other CO<sub>2</sub> capture technologies could greatly reduce the cost of meeting emissions reductions targets,<sup>2</sup> but would necessitate global capture on the order of 7 GtCO<sub>2</sub> per year or more by 2050.<sup>3</sup> Substantial

upscaling of BECCS is possible based on existing available biomass, while DAC which is only cost limited, can upscale rapidly in areas with cheap renewable energy resources, land, and water. In the last few years, commercial development of capture systems has increased rapidly,<sup>4</sup> but supporting the boom in capture will require deploying equal or greater annual CO<sub>2</sub> storage capacity where capture is occurring. In this paper, we investigate the possibility of using materials that can store CO<sub>2</sub> or carbon from CO<sub>2</sub>, even temporarily, to supplement geologic storage.

Upscaling CO<sub>2</sub> storage is nontrivial and has been hampered by the slow arduous regulatory and construction processes involved in bringing permanent geologic sequestration projects online. Geologic storage capacity is plentiful, but geographically limited and commercial capacity has remained relatively stable at approximately 40 MtCO<sub>2</sub> per year.<sup>4</sup> Ringrose and Meckel suggest that necessary injection well development, on the order of 10–14 thousand wells by 2050, is not outside of

Energy Analysis and Environmental Impacts Division, Lawrence Berkeley National Laboratory, Berkeley, CA, 94720, USA. E-mail: hannabreunig@lbl.gov

† Electronic supplementary information (ESI) available. See DOI: <https://doi.org/10.1039/d2ee03623a>



what has been historically achieved through petroleum exploitation, but relies heavily on undeveloped offshore regions and subsequent CO<sub>2</sub> shipping or pipeline delivery.<sup>5,6</sup> Several large projects are now under development, such as the Northern Lights Project in Europe which proposes to use ships to transport liquid CO<sub>2</sub> to a terminal for pipeline transport at capacities of up to 1.5 million tonnes of CO<sub>2</sub> per year.<sup>7</sup> Even as offshore transport options come online, new pipeline or rail connections transporting CO<sub>2</sub> to shipping terminals are unlikely to be viable for small- to medium-scale capture facilities (120 tonnes CO<sub>2</sub> per day or less).<sup>8</sup>

Additionally, dozens of new and existing utilization pathways have been identified that use CO<sub>2</sub> directly or as a carbon feedstock for building materials, chemicals and fuels,<sup>9,10</sup> but most are limited in that: (1) CO<sub>2</sub> is released immediately upon use; (2) potential consumption of CO<sub>2</sub> is projected to be small and not easily collocated with capture facilities; and (3) resulting products do not yet meet cost parity with incumbent petroleum-based products. For example, CO<sub>2</sub> can be sequestered in cement and concrete materials *via* mineral carbonation. However, it is projected that the near-term implementation of CO<sub>2</sub> for cement production in the United States (US) would require transporting less than a kilo-tonne of CO<sub>2</sub> per year to over 8000 distributed production sites.<sup>11</sup> Carbon dioxide can also be stored semi-irreversibly for very long periods of time through the mineralization of natural or waste alkaline materials. These reactions achieve the ultimate goal of carbon sequestration and thus are excellent storage solutions, but reputable reviews suggest they will be limited by rates of reaction and starting materials in the near future.<sup>12,13</sup>

Despite the lack of storage options available, large-scale carbon capture and storage (CCS) continues to be included in possible response options to climate change. Shared socio-economic pathways (SSP) are one such example where possible socio-political, economic, and technological changes and their climate implications are modeled.<sup>14</sup> As depicted in Fig. 1A, demand for CO<sub>2</sub> storage surpasses 2 GtCO<sub>2</sub> per year by 2035 in pathways where countries adopt a wide range of aggressive emissions reduction policies and reliance on CCS is minimal (SSP1 and SSP2).<sup>15</sup> In comparison, the necessary supply of storage from geologic storage and CO<sub>2</sub> utilization with meaningful carbon retention will not occur until after 2045.<sup>4,5,16</sup> This simple representation suggests that the gap in storage supply will be massive, at 2–10 GtCO<sub>2</sub> per year, but will only last for a few decades (Fig. 1B). As such, temporary reversible storage solutions that act as “batteries” for CO<sub>2</sub> may be of interest. We estimate the total amount of storage capacity and duration required for storage systems based on a physical process or material that releases the CO<sub>2</sub> or “self-discharges” on relatively short timescales, such as 3 or 10 years (Fig. 1B). Additional capture and storage would be required, compared with the SSP baselines, to compensate for self-discharge, which would ideally occur in a controlled measurable manner, unlike the gradual loss of carbon stored in biomass, biochar, or construction materials. Similar to the way a battery revolutionized society despite its cost and inevitable self-discharge, we see

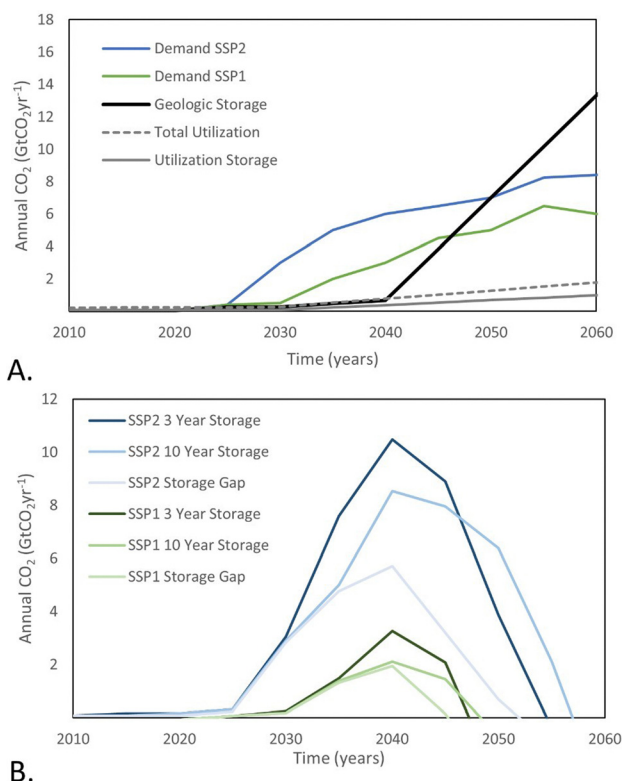


**Fig. 1** (A) Demand for CO<sub>2</sub> storage across scenarios towards limiting global mean temperature rise to 2 degrees warming (SSP1 and SSP2), plotted with historical and projected rates of supply of CO<sub>2</sub> storage. The geologic storage projection is based on proposed storage capacity under development out to 2040, and on optimistic but feasible injection well development rates (Scenario F from Ringrose & Meckel).<sup>5</sup> The utilization storage projection is based on CO<sub>2</sub> consumption for enhanced oil recovery, plastics and building materials; the projection for total utilization is plotted as a reference, and includes these applications as well as chemicals and fuels. (B) Gap in annual CO<sub>2</sub> storage capacity for SSP1 and SSP2 plotted with required storage capacity for systems that offer 3 or 10 years of storage.

great value in methods of storage that offer temporary storage of CO<sub>2</sub>, not for commercial use, but for the sole purpose of meeting near-term target removal rates in the first-half of the century. As such, unlike previous reviews of CO<sub>2</sub> conversion and utilization, in the context of CO<sub>2</sub> storage, we consider a much broader range of materials, as we are not concerned with future commercial value.

Currently, storing CO<sub>2</sub> in its molecular form without any chemical conversion at reasonable sizes for transportation or stationary storage involves compressing and/or cooling the gas. At standard ambient pressure and temperature, 1 tonne of CO<sub>2</sub> has a volume of 506 m<sup>3</sup>, which can be imagined as a cube with sides as long as a bus. Industries already transport gaseous or liquid CO<sub>2</sub> by truck, ship, rail, or pipeline, with conditions presented in Fig. 2. Condensed liquid CO<sub>2</sub> is typically stored at 238 to 261 K at 1.2–2.5 MPa with densities between 993–1096 kg m<sup>-3</sup>. Liquid CO<sub>2</sub> transport ships such as the Coral Carbonic offer capacities between 1200–1500 m<sup>3</sup> while larger ships proposed by Daewoo Shipbuilding & Marine Engineering



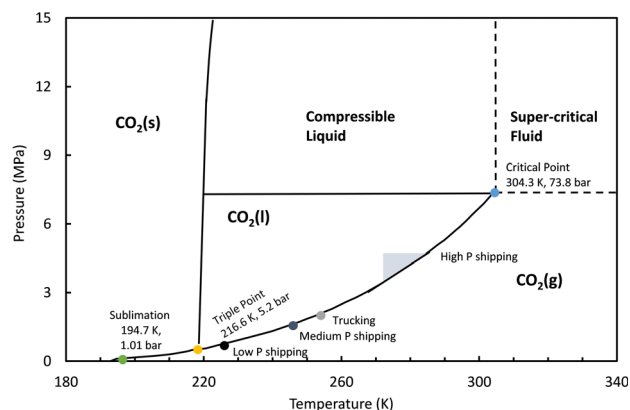


Fig. 2 Carbon dioxide phase diagram with pressure and temperature conditions for commercial and state of the art storage and transport modes.

offer capacities as large as  $100\,000\text{ m}^3$ .<sup>17,18</sup> New state of the art ships proposed by Knutsen NYK Carbon Carriers have moved towards ambient temperature and high pressure (4.5 MPa) liquid storage to boost capacity.<sup>19</sup> Despite these demonstrations of large-scale liquefaction, it is limited in that it requires expensive specialized tanks, energy intensive liquefaction processes, and offers limited storage durations (days) due to boil-off issues. Compressed  $\text{CO}_2$  can be achieved at moderate pressures, but storing  $\text{CO}_2$  for long periods in pressurized tanks presents safety and physical footprint concerns. Furthermore, just drying and compressing  $\text{CO}_2$  for pipeline transport (7.5 MPa) may require more electricity (256–475 kW h per t $\text{CO}_2$ ) than reported minimum mole-specific work for separating  $\text{CO}_2$  from air (e.g. Carbon Engineering: 130 kW h per t $\text{CO}_2$  or amine capture 380 kW h per t $\text{CO}_2$ ).<sup>20–22</sup> Solid  $\text{CO}_2$ , commonly referred to as “dry ice” is used in industry for short duration refrigeration, but it is not used for long duration storage or transportation. We do not consider compressed gas or dry ice storage further in this analysis.

Storage of  $\text{CO}_2$  using a material, however briefly, is already the motivation of DAC and other point-source  $\text{CO}_2$  capture technologies that rely on a material to separate  $\text{CO}_2$  from other gases. Liquid and solid materials in these systems have been extensively studied for carbon capture, but not for temporary  $\text{CO}_2$  storage applications. A class of solids well known for their ability to store  $\text{CO}_2$  are carbonate salts, including alkali metal and alkaline earth metal carbonates. If stored properly, carbonate salts can retain  $\text{CO}_2$  at ambient conditions for months or years. In theory, carbonates could offer permanent storage, but in practice storage duration is affected by material morphology, and not just chemical stability. For example, solids need to maintain their powdery character in order to enable loading and transport to a final storage or utilization end-use. Carbonate salts are widely utilized in cement,<sup>23</sup> paper and pulp,<sup>24</sup> and iron and steel industry<sup>25</sup> as a chemical feedstock, and more recently as chemical intermediates in proposed aqueous and mineral carbonation-based DAC processes by companies such as Carbon Engineering<sup>20</sup> and Heirloom.<sup>26</sup> In these cases,  $\text{CO}_2$

storage *via* carbonate salts may be leveraged in these existing and forthcoming processes with minor modifications.

Advanced porous materials such as zeolites, mesoporous silica, polymeric resins, activated carbon, and rigid and flexible metal organic frameworks (MOF) are another material class that have been investigated in the separation of  $\text{CO}_2$  from ambient air and flue gases.<sup>27</sup> Porous materials offer large internal surface areas with amine functionalized groups to which  $\text{CO}_2$  can selectively and reversibly bind.<sup>28</sup> These materials are being tuned to minimize the energy required to take  $\text{CO}_2$  off (*i.e.* regeneration), while remaining selective to  $\text{CO}_2$  over other compounds such as water. This challenge is key to outcompeting energy intensive absorptive liquids such as monoethanolamine, and achieving this balance while ensuring the material can take up  $\text{CO}_2$  at high densities has yet to be achieved for DAC. Still, existing materials today have demonstrated higher densities than what is achieved by compressed gas tanks at the same pressure.<sup>27</sup> This is an active area of research, and new materials and design considerations may lead to breakthroughs in performance.

A third class of materials that could be used to store  $\text{CO}_2$  is liquid organic hydrogen carriers (LOHC) with high carbon contents, include ethanol, methanol, formic acid (FA), formate salts (FS), and other hydrocarbons. These carriers can be dehydrogenated at elevated temperatures with a catalyst to deliver high purity  $\text{H}_2$ , the status of which is thoroughly discussed by Southall and Lukashuk.<sup>29</sup> While well established, generating these materials directly from  $\text{CO}_2$  requires new approaches, such as electrochemical processes. Furthermore, the use of  $\text{CO}_2$  as a material to store  $\text{H}_2$  has been well studied, but never from the perspective of  $\text{CO}_2$  storage. This might change if the value of mitigating or capturing a tonne of  $\text{CO}_2$  is higher than the value of delivering the stored hydrogen. The availability of affordable  $\text{H}_2$  is considered a key assumption in the projected growth of  $\text{CO}_2$  utilization pathways for fuel and chemical development, and is reflected in our projections of future demand for  $\text{CO}_2$  storage.

We believe reversibility of storage is an acceptable and even beneficial aspect of the materials evaluated for several reasons. As we envision these storage systems to be only temporary “last resort” solutions that may take up large amounts of land, reversibility offers the possibility of decommissioning and later use of the  $\text{CO}_2$  and storage material. Ideally reversibility is a controlled process, but even a material that exhibits gradual release of  $\text{CO}_2$  could be of value if it is ready to be deployed and helps us achieve significant near-term capture. Finally, reversibility allows for materials to double as carriers of  $\text{CO}_2$  for transportation.

In this study, we screen materials based on gravimetric (*i.e.*  $\text{CO}_2$  mass fraction,  $\text{CO}_2$  wt%) and volumetric  $\text{CO}_2$  capacities (*i.e.*  $\text{CO}_2$ -density), stability, and the energetics of getting  $\text{CO}_2$  on and off materials. We focus on materials that can offer high densities of  $\text{CO}_2$  to minimize material requirements. Overcoming the low volumetric density of  $\text{CO}_2$  at ambient conditions ( $1.98\text{ kg m}^{-3}$ ) will be necessary to reduce the number of tanks and land required for storage. The storage methods included in this study are: carbonate salts, sorbents,



liquid organic carriers, and chemical solids that allow for reversible CO<sub>2</sub> storage. We estimate the material required and land footprint of multi-year storage. While the focus of this paper is on the storage of CO<sub>2</sub>, we include a perspective on the use of materials for truck transportation of CO<sub>2</sub>.

## Methods and materials

The feasibility of CO<sub>2</sub> storage was estimated for materials in each class. Upon down selection, candidates were evaluated for CO<sub>2</sub> capture facilities with capacities of 10 tonnes per year (tpy) and 1 million tonnes per year (Mtpy), which are scales typically used to represent pilot and large DAC facilities. The source could be a facility that generates CO<sub>2</sub> as a by-product or captures it from a waste stream, or a dedicated CO<sub>2</sub> removal facility such as DAC. We note that some materials evaluated capture CO<sub>2</sub> directly in the process of storage, which obviates the need for a CO<sub>2</sub> source.

### Screening method

We start by conducting a broad screening of material classes that can store CO<sub>2</sub> or carbon from CO<sub>2</sub> through adsorption or chemical bonds. As gleaned from research on H<sub>2</sub> carriers, there are a number of properties to consider when selecting a storage material.<sup>30</sup> These include properties such as safety, toxicity, compatibility with existing infrastructure, total cost of ownership, material availability, storage duration, storage capacity, reversibility, material durability/cyclability, energy efficiency, and life cycle impacts. As many of the materials evaluated in this analysis have yet to be properly explored for CO<sub>2</sub> storage and transport, there are a number of data gaps limiting the ability to estimate these properties. As such we kept our initial screening to general assessments of technology maturity, stability, reversibility, energetics, and CO<sub>2</sub> capacity, which we define as:

$$\rho_{\text{CO}_2} = \frac{m_{\text{CO}_2 \text{ stored in compound}}}{m_{\text{compound}}} \cdot \rho_{\text{compound}} \quad (1)$$

where  $m$  is mass in kg and  $\rho$  is the density in kg m<sup>-3</sup>. Volumetric capacity indicates how densely CO<sub>2</sub> can be stored and influences the volume of the storage unit. In packed powder or sorbent materials, bulk storage capacity is less than the volumetric capacity of the sorbent, as it includes inter-particle void volume, which can be influenced by method of packing, while crystal or particle density is an intrinsic property.

Gravimetric capacity is the quantity of CO<sub>2</sub> stored within a unit mass of material and is of major relevance to transportation applications which in many cases are weight limited. It is important to note that a fair comparison of material storage options with compressed gas or liquid CO<sub>2</sub> storage will include the additional weight and volume of the containers used, as is done in this study.

For sorbents, we modelled storage tanks filled with porous packing material (pellets made of crystal sorbent material) as packed beds. The mass of sorbent material within the container is estimated using (eqn (2)) where  $\rho_s$  is the single crystal density in kg m<sup>-3</sup> and  $\varepsilon$  is the porosity of the pellet or tank bed. Unlike

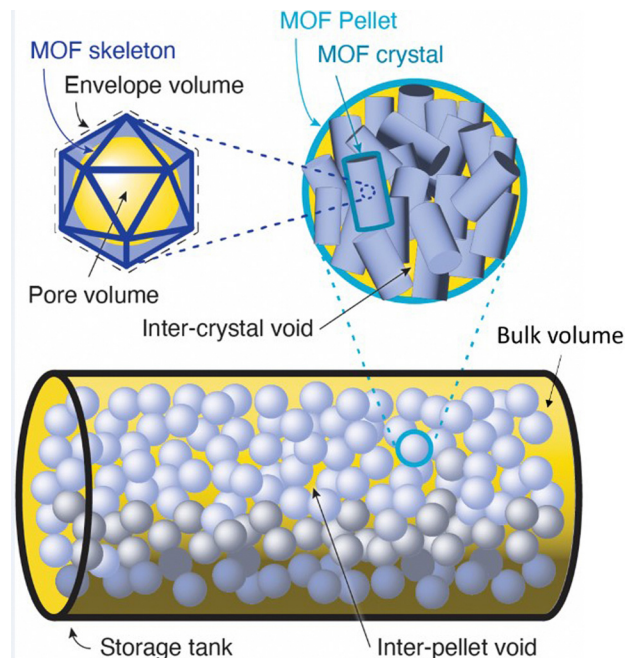


Fig. 3 Illustration demonstrating bulk volume used for estimating bulk density of the MOF-packed tank, pellet volume and inter-crystal void volume included in pellet porosity, and crystal pore and skeletal volumes.

skeletal density, which is the ratio of the mass of crystal solid to the volume of the solid excluding pore volume, crystal density divides the same mass of crystal solid by the envelope volume of the crystal, giving a much lower density (Fig. 3). In this analysis, the porosity of the pellet and bed are used to derive the inter-crystal and inter-pellet pore volumes, respectively, and exclude crystal pore volume which is evaluated separately.

The CO<sub>2</sub> stored inside the crystal envelope volume of the sorbent  $q_{\text{CO}_2}^{\text{compound}}$  in kg-CO<sub>2</sub> per kg-material includes CO<sub>2</sub> adsorbed on the material surface and CO<sub>2</sub> stored in the pore volume (eqn (3)) where  $V$  is the pore volume in m<sup>3</sup> kg<sup>-1</sup> and  $\rho_{\text{gasCO}_2}$  is the CO<sub>2</sub> gas density in kg m<sup>-3</sup>. The CO<sub>2</sub> stored in the tank is the combination of  $q_{\text{CO}_2}^{\text{compound}}$ , the CO<sub>2</sub> in the inter-crystal void inside the pellets, and the CO<sub>2</sub> in the inter-pellet void space at a specific temperature and pressure (eqn (4)). The amount adsorbed and in the pore volume at a given temperature and pressure is derived from experimental isotherm data, which tend to be reported for crystals at conditions relevant to CO<sub>2</sub> capture (0.1 MPa or lower). The absolute amount of CO<sub>2</sub> storage with adsorbents in a tank can be maximized by increasing the pressure, which is limited to around 6.4 MPa at 298 K due to liquefaction.

$$\rho_{\text{bulk}} = \rho_s(1 - \varepsilon_{\text{pellet}})(1 - \varepsilon_{\text{bed}}) \quad (2)$$

$$q_{\text{CO}_2}^{\text{compound}} = \frac{m_{\text{CO}_2 \text{ sorbed to compound}}}{m_{\text{compound}}} + V \cdot \rho_{\text{gasCO}_2} \quad (3)$$

$$\rho_{\text{CO}_2} = q_{\text{CO}_2}^{\text{compound}} \cdot \rho_{\text{bulk}} + \rho_{\text{gasCO}_2} \cdot (1 - \varepsilon_{\text{bed}})\varepsilon_{\text{pellet}} + \rho_{\text{gasCO}_2} \cdot \varepsilon_{\text{bed}} \quad (4)$$





A number of materials identified were too early stage or do not meet our screening criteria. We provide additional details on these materials in the ESI† to guide future work in this space. For solid and liquid carriers, we define four levels of technology maturity: L1: neither CO<sub>2</sub> fixation nor regeneration are commercial; L2: either fixation or regeneration is commercial; L3: fixation and regeneration are commercial but require validation for storage; and L4: commercially used. For sorbents, as the reactor design for CO<sub>2</sub> storage may be similar to existing concepts for compressed gas storage, the biggest bottleneck is likely to be materials synthesis. As such, we define four levels of technology maturity as: L1: a theoretical concept; L2: lab-scale synthesis of material; L3: demonstration for DAC; and L4: industrial-scale synthesis.

### Truck transport model

We estimated the energy associated with transporting CO<sub>2</sub> by road for each candidate material and for liquified CO<sub>2</sub> assuming long haul commercial trucks with B-train configuration that comprises a tractor and two trailers. We assume liquid CO<sub>2</sub> is transported at 2.2 MPa and 255 K, giving a bulk density of 1022 kg m<sup>-3</sup>. Tare weight, or empty weight of the truck without material is the sum of the tractor and trailer weights, which is 21.0, 18.0, and 19.3 tonnes for trucks designed for compressed gas (including cryogenic liquid CO<sub>2</sub>), liquids, and solids, respectively. We assumed trucks are filled until either the United States federal limit on gross weight rating of the truck (70.0 tonnes) or the volume limit of the trailer (84.7 m<sup>3</sup>) is met. For perspective, commercial trucks transport CO<sub>2</sub> in small quantities of 2–30 tonnes, while rail cars can transport larger quantities ~60 tonnes but are limited to rail networks.

Upon delivery of the CO<sub>2</sub>, we assumed trucks will return to the CO<sub>2</sub> capture facility either empty (in the case of liquid CO<sub>2</sub>, liquid organic carriers or other one-way carriers), or with the regenerated material. Trucks were assumed to travel on ungraded highway networks at a fixed speed of 100 km h<sup>-1</sup>, which is reflective of speed limits for freight trucks in the United States and in the European Union (80–130 km h<sup>-1</sup>). The energy needed for trucking was calculated based on the energy needed to overcome the rolling resistance and aerodynamic drag of a typical heavy-duty truck.<sup>31</sup> We then assumed an engine and transmission efficiency of 40% and 90%, respectively. Total energy required takes into account the mass of the transported CO<sub>2</sub>, the material, and the tare weight of the B-Train on the outbound and inbound trips.

For the MOF-filled trailers, we assumed CO<sub>2</sub> is transported at 5.6 MPa and 98–99% of CO<sub>2</sub> is discharged upon arrival. This reflects a scenario where pressure is decreased to 0.03 MPa. Thermophysical properties of CO<sub>2</sub> are retrieved from National Institute of Standards and Technology (NIST) Chemistry WebBook.<sup>32</sup> Loading trucks with solid powders or stable liquids, as would be the case for solid and liquid carriers, at ambient conditions will not require significant energy, but the chemical conversion of CO<sub>2</sub> to a carrier likely will. As significant uncertainty remains regarding the supply chain logistics of chemical solid and liquid carriers, we believe it would be too

preliminary to present results for charging and discharging across material classes.

### Pipeline model

Today, there are over 6500 km of CO<sub>2</sub> pipelines worldwide, transporting approximately 68 million tonnes of CO<sub>2</sub> per year.<sup>33</sup> Pipelines are designed to keep CO<sub>2</sub> in either a gaseous, dense liquid, or supercritical phase, and CO<sub>2</sub> is typically compressed to pressures above 7.5 MPa to avoid two-phase flow regimes and changes in compressibility at temperatures of the surrounding soil. Because CO<sub>2</sub> cannot exist as a liquid at atmospheric conditions, it takes pressurization and cooling to achieve a liquid state. Supercritical CO<sub>2</sub> storage is based on compression to 10.0–15.2 MPa at 313 K. Supercritical pipelines are used when moving large quantities of CO<sub>2</sub> over a long distance. The high density of the supercritical CO<sub>2</sub> (629–783 kg m<sup>-3</sup>), which is comparable to liquid phase, allows for a high throughput transport while its low viscosity (48–69 μPa s), similar to vapor state, helps reduce friction loss during transport.

Numerous models for estimating pipeline pressure drop and necessary pipeline diameters exist, but real-world examples of CO<sub>2</sub> pipelines suggest design and operation is highly location dependent and requires proper engineering especially for dense state CO<sub>2</sub>.<sup>34,35</sup> As such, we used values from a similar-scale (12 inch diameter) hypothetical pipeline and assumed recompression from 10.3 to 15.2 MPa at 313 K is required every 100 km (49 Pa m<sup>-1</sup> pressure drop), to avoid pressure falling below 10.3 MPa.<sup>36</sup> From this, we derived a single-stage recompression energy (14.7 kJ per kg-CO<sub>2</sub>) using the Peng–Robinson equation of state in ProSim software, assuming a 98% mechanical efficiency, 97% electrical efficiency, 65% isentropic efficiency, and 10% additional power consumption for auxiliaries. This is much lower than the initial compression required to take gaseous CO<sub>2</sub> from 0.1 MPa to a supercritical state. For example, Climeworks derives a 363.3 kJ per kg-CO<sub>2</sub> compression energy assuming an 8 stage compression and intercooling system is used to take CO<sub>2</sub> from 0.1 to 15.0 MPa at 313 K.<sup>37</sup> Carbon Engineering derives a 475.2 kJ per kg-CO<sub>2</sub> compression energy assuming a 4 stage compression system is used to take CO<sub>2</sub> to 15.2 MPa at 313 K.<sup>20</sup> Neither report recompression energy for pipelines. These compression energies match well with that reported by the Carbon Capture Simulation Initiative Toolset implemented in Aspen Plus for the conditioning of ambient pressure CO<sub>2</sub> to 15.2 MPa (370–441 kJ per kg-CO<sub>2</sub>).<sup>38</sup> We find our approach for estimating recompression energy to be reasonable as we were able to derive similar compression energies of 392 to 420 kJ per kg-CO<sub>2</sub> assuming 4 and 3 stage compression, respectively.

### CO<sub>2</sub> emissions from transport

Emissions during transport are estimated by accounting for the emission factor of diesel fuel (0.07 kgCO<sub>2</sub> per MJ) for trucking<sup>39</sup> and the national grid carbon intensity in the US in 2020 (0.38 kg kW<sup>-1</sup> h<sup>-1</sup> or 0.107 kgCO<sub>2</sub> per MJ)<sup>40</sup> for pipeline recompression. Based on this, we estimated a breakeven distance for all options where CO<sub>2</sub> emissions generated during



transport are equal to the quantity of CO<sub>2</sub> being transported. Note that these estimations are based on first-order calculations to compare different CO<sub>2</sub> carrier options and the more accurate emissions estimations would require dedicated life-cycle assessment for each option.

### Stationary storage analysis

Gravimetric and volumetric capacities were used to estimate the necessary storage material, total weight, and total volume required for the pilot facility and regional hub scenarios, assuming perfect conversion for chemical solid and liquid storage. As MOFs require temperature and pressure maintenance, we excluded them from long-duration stationary storage. Typical storage equipment used in the fossil fuel industry for powder solids, flammable liquids, and liquid CO<sub>2</sub> were assumed. Specifications of storage silos or tanks assumed for the small- and large-scale storage systems are included in Table S1 (ESI<sup>†</sup>). Physical footprint was estimated based on the storage equipment diameter plus spacing of tanks based on NFPA 30 safety codes. This value was divided by the stored CO<sub>2</sub> to estimate land footprint intensities in units of m<sup>2</sup> per tCO<sub>2</sub>.

## Results and discussion

### Sorbent carrier potential

Solid porous adsorbents have been extensively studied and developed to separate CO<sub>2</sub> from dilute sources where CO<sub>2</sub> concentrations are typically below 30% and as low as 0.04% if capturing from ambient air. This requires sorbents to have high CO<sub>2</sub> selectivity and uptake capacity as well as fast kinetics at sub-atmospheric partial pressure which typically requires surface functionalization with alkaline molecules such as amines. Implicit in these parameters are other critical parameters such as the enthalpy of adsorption of CO<sub>2</sub>, which determines both the selectivity and energy required for regeneration. Binding CO<sub>2</sub> too strongly may enhance selectivity and kinetics of adsorption but can lead to costly regeneration. While there are many types of porous materials under investigation for CO<sub>2</sub> capture, we identified MOF,<sup>41</sup> activated carbon,<sup>42</sup> and zeolite<sup>43,44</sup> adsorbents that have CO<sub>2</sub> uptake data at pressures greater than 3 MPa at near room temperature. The properties of the identified adsorbents are shown in Table 1. A number of materials can adsorb CO<sub>2</sub> at high temperatures, including CaO and MgO, which are discussed in the following section, hydrotalcites, and lithium-based materials.<sup>45</sup> We do not provide further details due to their expected high costs.

### Zeolites

Zeolites are porous aluminosilicate materials that have relatively low material costs, very high stability and have demonstrated rapid adsorption and low energy penalties in post-combustion applications.<sup>27</sup> Zeolite 13x is commercially available and has an excess CO<sub>2</sub> uptake, which is defined as the amount of CO<sub>2</sub> bonded to the surface and can be thought of as the gravimetric capacity, of 0.16 g g<sup>-1</sup> at 4.5 MPa (excluding void spaces).

**Table 1** Physical characteristics and measured CO<sub>2</sub> uptake data of candidate adsorbents at 25 °C. Max P: maximum pressure a measurement was taken at. SA: surface area

Sorbent	BET SA m <sup>2</sup> /g	Pore volume cm <sup>3</sup> /g	Max P MPa	Excess uptake g/g	Maturity Level	Ref
Zeolite 13X	355–392	0.14	4.5	0.16	4	44
AC Norit R1 extra	1450	0.47	3	0.45	4	43
AC Maxsorb	3250	1.79	4.6	1.18	4	43
MOF-200	4530	3.59	5.7	2.39	2	42
MOF-210	6240	3.6	5.6	2.37	2	42

The reference values shown in Table 1 are based on the NIST reference zeolite material, ammonium ZSM-5 zeolite. The measured values are based on a standardized high-pressure CO<sub>2</sub> measurement, harmonizing results across measurement techniques and procedures being practiced. Notably, zeolites have been challenged by the presence of water, where CO<sub>2</sub> adsorption capacity drops over time as water competes for binding sites. As such, research has focused on how to add highly charged species on the surface to increase affinity for CO<sub>2</sub>, such as alkali and alkaline earth metal cations.<sup>46</sup> Future research for tuning zeolites for storage applications would need to study whether the lack of water may lead to higher cycling capacity and whether this increase in affinity subsequently increases the energy required for regeneration.

### Activated carbon

Enhanced activated carbons are amorphous porous forms of carbon that have low material costs, very high surface areas, and require relatively low temperatures for regeneration. Overcoming the relatively low capacities of CO<sub>2</sub> at low pressure has been a focus for separation applications, however, due to the high surface areas, activated carbons can have very high CO<sub>2</sub> capacities at higher pressures that would be used for storage applications.<sup>47</sup> That being said, predicting performance at specific conditions from result reported in literature is challenging as reporting methods are not standardized and the correlation between surface chemistry and capacity is still not well understood. Maxsorb, a commercially available high-surface area activated carbon, has the highest surface area and CO<sub>2</sub> adsorption at elevated pressure amongst activated carbon as shown in Table 1.

### Metal–organic frameworks

Metal–organic frameworks consist of metal-based nodes bridged by organic linking groups to form a network. They have ultra-high surface areas compared to the materials just discussed, and have highly tuneable structures and surface chemistries. In particular, tuning structures in the M<sub>2</sub>(dobdc)(M = Mg, Mn, Fe, Co, Ni, Zn) series has been an area of focus for CO<sub>2</sub> capture. The highest excess CO<sub>2</sub> uptake has been demonstrated relatively recently in MOF-200 and MOF-210 structures. MOF-210 has an ultrahigh



surface area of  $6240 \text{ m}^2 \text{ g}^{-1}$  and a crystal pore volume of  $3.6 \text{ cm}^3 \text{ g}^{-1}$ .<sup>41</sup> The volume-specific internal surface area ( $2060 \text{ m}^2 \text{ cm}^{-3}$ ) nears for the ultimate adsorption limit for solid materials. Unlike zeolites which have degraded performance in the presence of water, MOFs show increased chemical stability in the presence of steam. Carbon dioxide storage could be an attractive application for MOFs due to their high capacities, however, several challenges must be overcome, including high material costs and potentially weak mechanical strength.

### Down-selection of sorbents

Future experimental work is needed to characterize material performance as some key challenges, such as amine degradation for MOFs, low uptake at low pressures for activated carbons, or low uptake in the presence of water for zeolites, may not arise in storage applications. Still, sorbents offer better capacities than compressed gas tanks.

For the analysis, we selected MOF-210 which uses an octahedral metal-ion cluster ( $\text{Zn}_4\text{O}(\text{CO}_2)_6$ ) with 4,4',4''-[benzene-1,3,5-triyl-tris(ethyne-2,1-diyl)]tribenzoate (BTE) and biphenyl-4,4'-dicarboxylate (BPDC) linkers to serve as a representative material due to the availability of single-component gas adsorption isotherm data for making predictions on  $\text{CO}_2$  uptake under higher pressures. MOF-200 has also been demonstrated for  $\text{CO}_2$  separation, but was not considered for transport and storage due to its instability that limits its cyclic use. At 298 K, the density of gaseous  $\text{CO}_2$  is  $1.8\text{--}162 \text{ kg m}^{-3}$  between  $0.1\text{--}5.6 \text{ MPa}$  without adsorbents. The total  $\text{CO}_2$  density inside the volume increases to  $6\text{--}436 \text{ kg m}^{-3}$  at the same pressure if MOF-210 pellets are used to facilitate  $\text{CO}_2$  uptake through adsorption. While at this operational range, the volumetric storage capacity of MOF-210 is larger than compressed  $\text{CO}_2$ , it remains smaller than conventional approaches of storing  $\text{CO}_2$  at liquid or supercritical state. However, storing  $\text{CO}_2$  at liquid or supercritical state comes with higher energy demand due to heating/cooling as well as compression requirements. Thus, adsorbents may provide a more energy-efficient storage solution if the  $\text{CO}_2$  capacity can be further improved.

A theoretical upper bound of  $\text{CO}_2$  uptake of adsorbents can be estimated by assuming the crystal pore space can be saturated with  $\text{CO}_2$  *via* condensation, so that the density of  $\text{CO}_2$  in the pore volume reaches the density of liquid  $\text{CO}_2$ . We refer to this hypothetical case as future MOF. The total  $\text{CO}_2$  uptake using future MOF is estimated by adjusting the  $\text{CO}_2$  density inside the pore volume of MOF-210 with a multiplier so that the  $\text{CO}_2$  density inside the pore volume at  $5.6 \text{ MPa}$  reaches that of liquid  $\text{CO}_2$  at around  $730 \text{ kg m}^{-3}$ . This is equivalent to increasing the absolute quantity of adsorbed  $\text{CO}_2$  on MOF-210 by 69%. While increasing the uptake capacity of adsorbents is not a trivial task, this simplified example illustrates potential benefits of adsorbent-based  $\text{CO}_2$  storage.

### Chemical solid carbon dioxide carrier potential

Chemical solid  $\text{CO}_2$  carriers are discussed in this section and classified as alkali carbonates, alkaline earth metal carbonates, and other non-sorbent chemical solids. Properties of the

reviewed materials are provided in Table 2. Some of the most abundant elements found in the earth crust are silicon, aluminium, iron, titanium and manganese which makes them potentially interesting for storing and transporting large quantities of  $\text{CO}_2$  as carbonates. Also, ammonium is a common compound that forms carbonate and bicarbonate. However, none of these carbonates shows promising characteristics for temporary  $\text{CO}_2$  storage. A more detailed description of these materials and why they are not suitable for temporary  $\text{CO}_2$  storage is provided in the ESI.<sup>†</sup>

### Alkali carbonates

Lithium carbonate only exists in anhydrous form and has a solid density of  $2110 \text{ kg m}^{-3}$ , which results in a  $\text{CO}_2$  mass fraction of 59.6  $\text{CO}_2$  wt% and a  $\text{CO}_2$ -density of  $1257 \text{ kg m}^{-3}$  (in powder form this number is expected to decrease by roughly 50%). When heated to about  $800^\circ\text{C}$  (melting point  $723^\circ\text{C}$ )  $\text{Li}_2\text{CO}_3$  starts to decompose into  $\text{Li}_2\text{O}$ ; however, much higher temperatures are needed for complete conversion.<sup>48</sup> After regeneration,  $\text{Li}_2\text{O}$  can be used directly to capture  $\text{CO}_2$  or converted to  $\text{LiOH}$  which is used as a solid sorbent in submarines to capture  $\text{CO}_2$  from breathing air<sup>49</sup> or can be dissolved in water for gas scrubbing (similarly to industrial gas scrubbing process using  $\text{NaOH}$  or  $\text{KOH}$ ). Lithium hydroxide is an order of magnitude more soluble than  $\text{Li}_2\text{CO}_3$  ( $12.9 \text{ g L}^{-1}$ ) which can be recovered by precipitation or crystallization. This property and the formation of metastable  $\text{LiHCO}_3$  in aqueous solutions under slightly elevated  $\text{CO}_2$  partial pressures is industrially used in the Quebec process to obtain technical grade  $\text{LiCO}_3$ ;<sup>50</sup> however, is considered to be energy intensive.<sup>48</sup> Other regeneration processes for the release of  $\text{CO}_2$  after storage include the use of  $\text{Ca}(\text{OH})_2$  to produce  $\text{CaCO}_3$  and  $\text{LiOH}$ . Due to the hygroscopic nature of dry  $\text{Li}_2\text{CO}_3$ , it needs to be stored in a cool and dry environment and shelf life is limited to about 1–2 years. The chemistry around  $\text{LiHCO}_3$  is still not well understood and it is believed that the bicarbonate only exists as metastable ion in aqueous solutions.

Sodium carbonate has similar properties as  $\text{Li}_2\text{CO}_3$ . In its anhydrous form it has a solid density of  $2540 \text{ kg m}^{-3}$ . However, as sodium atoms are more than 3-times heavier than lithium atoms, this results in a 16% reduction in  $\text{CO}_2$ -density to  $1055 \text{ kg m}^{-3}$  (again, in powder form this number is expected to decrease by roughly 50%). The corresponding  $\text{CO}_2$  mass fraction is 41.5  $\text{CO}_2$  wt%. While the production and storage of  $\text{Na}_2\text{CO}_3$  is relatively straight forward – it can be obtained from the reaction of  $\text{NaOH}$  with air as commonly done in DAC systems<sup>51</sup> – the regeneration of  $\text{CO}_2$  from  $\text{Na}_2\text{CO}_3$  is challenging. Sodium carbonate does not thermally decompose into  $\text{CO}_2$  and  $\text{Na}_2\text{O}$  even at temperatures as high as  $2000^\circ\text{C}$  (very high reaction enthalpy  $319.3 \text{ kJ mol}^{-1}$ ). Instead  $\text{Ca}(\text{OH})_2$  can be used to restore the  $\text{NaOH}$  while producing  $\text{CaCO}_3$  which can be separated and thermally decomposed into  $\text{CaO}$  and  $\text{CO}_2$  (more discussion about this reaction later).<sup>51</sup> Depending on the regeneration logistics with  $\text{Ca}(\text{OH})_2$ , the  $\text{CO}_2$  can be stored as either  $\text{Na}_2\text{CO}_3$  or  $\text{CaCO}_3$ . The use of  $\text{Ca}(\text{OH})_2$  for  $\text{CO}_2$  recovery from the absorbent has been successfully demonstrated and is



Table 2 Key physiochemical properties of solid and liquid chemical carriers for CO<sub>2</sub>

	Density kg/m <sup>3</sup>	Solubility g/L (25°C)	CO <sub>2</sub> Mass Fraction wt.-%	CO <sub>2</sub>		Decarbonization Product		Reaction Enthalpy kJ/mol	Reaction T °C	Shelf Life Years	Maturity Level	Hazard Information
				Density kg/m <sup>3</sup>	Product Name							
Li <sub>2</sub> CO <sub>3</sub>	2110	12.9		59.6	1257	Li <sub>2</sub> O		223.8	800-1300	1-2	2	H302, H319
LiHCO <sub>3</sub>	Metastable: Only Exists in Aqueous Solution											
Na <sub>2</sub> CO <sub>3</sub>	2540	340.7*		41.5	1055	Na <sub>2</sub> O		319.3	No Reaction	2-3	3	H319
Na <sub>2</sub> CO <sub>3</sub>	2540	340.7*		41.5	1055	NaOH (with Ca(OH) <sub>2</sub> )		-2.0†	Ambient	2-3	3	H319
Na <sub>2</sub> CO <sub>3</sub> · H <sub>2</sub> O	2250	423.1*		35.5	799	Na <sub>2</sub> CO <sub>3</sub> (drying)			100-200	>3		H319
Na <sub>2</sub> CO <sub>3</sub> · 7H <sub>2</sub> O	1510	1254.6*		19.0	286	Na <sub>2</sub> CO <sub>3</sub> · H <sub>2</sub> O (drying)			35	>3		H319
Na <sub>2</sub> CO <sub>3</sub> · 10H <sub>2</sub> O	1460	2185.3*		15.4	225	Na <sub>2</sub> CO <sub>3</sub> · 7H <sub>2</sub> O (drying)			32	>3		H319
NaHCO <sub>3</sub>	2200	96.0*		26.2	576	Na <sub>2</sub> CO <sub>3</sub>		135.5	100-200	2-3	3	None
NaHCO <sub>3</sub>	2200	96.0*		52.4	1153	NaOH (with Ca(OH) <sub>2</sub> )		-9.4†	Ambient	2-3	3	None
K <sub>2</sub> CO <sub>3</sub>	2430	1103.0*		31.8	774	K <sub>2</sub> O		393.5	No Reaction	1-5	2	H302, H315, H319, H335
K <sub>2</sub> CO <sub>3</sub>	2430	1103.0*		31.8	774	KOH (with Ca(OH) <sub>2</sub> )		-3.5‡	Ambient	1-5	2	H302, H315, H319, H336
K <sub>2</sub> CO <sub>3</sub> · 3/2H <sub>2</sub> O	2420	1635.0*		26.6	645	K <sub>2</sub> CO <sub>3</sub> (drying)			200-350	2-Inf		H302, H315, H319, H335
KHCO <sub>3</sub>	2170	224.0*		22.0	477	K <sub>2</sub> CO <sub>3</sub>		140.9	100-120	2-Inf	2	H315, H319, H335
KHCO <sub>3</sub>	2170	224.0*		44.0	954	KOH (with Ca(OH) <sub>2</sub> )		-5.11‡	Ambient	2-Inf	2	H315, H319, H335
MgCO <sub>3</sub>	2958	0.1		52.2	1544	MgO		116.9	360-800	3-Inf	3*	None
MgCO <sub>3</sub> · 2H <sub>2</sub> O	2825	0.2		36.6	1033	MgCO <sub>3</sub> (drying)			179-300	3-Inf		None
MgCO <sub>3</sub> · 3H <sub>2</sub> O	1837	0.2		31.8	584	MgCO <sub>3</sub> · 2H <sub>2</sub> O (drying)			157-300	3-Inf		None
MgCO <sub>3</sub> · 5H <sub>2</sub> O	1730	0.3		25.2	437	MgCO <sub>3</sub> · 3H <sub>2</sub> O (drying)			Ambient	3-Inf		None
Mg(HCO <sub>3</sub> ) <sub>2</sub>	Metastable: Only Exists in Aqueous Solution											
CaCO <sub>3</sub>	2830	< 0.1		44.0	1244	CaO		178.4	650-1050	2-Inf	4	None
Ca(HCO <sub>3</sub> ) <sub>2</sub>	Metastable: Only Exists in Aqueous Solution											
SrCO <sub>3</sub>	3500	< 0.1		29.8	1043	SrO		234.5	875-1035	3-Inf	1	None
Sr(HCO <sub>3</sub> ) <sub>2</sub>	Metastable: Only Exists in Aqueous Solution											
BaCO <sub>3</sub>	4286	< 0.1		22.3	956	BaO		243.5	1350	3-Inf	1-2	H302
Ba(HCO <sub>3</sub> ) <sub>2</sub>	Metastable: Only Exists in Aqueous Solution											
SiCO <sub>4</sub>	Unstable											
Al <sub>2</sub> (CO <sub>3</sub> ) <sub>3</sub>	Metastable: Only Exists in Aqueous Solution											
FeCO <sub>3</sub>	3900	< 0.1		38.0	1482	Fe <sub>3</sub> O <sub>4</sub>		77.8	500-733	2-5	1	None
TiCO <sub>3</sub> /Ti(CO <sub>3</sub> ) <sub>2</sub>	Unstable											
MnCO <sub>3</sub>	3120	< 0.1		38.3	1195	MnO		103.2	100-300	2-Inf	1	None
(NH <sub>4</sub> ) <sub>2</sub> CO <sub>3</sub>	1500	250		45.8	687	NH <sub>3</sub>			58	1-2	2*	H302, H319
(NH <sub>4</sub> )HCO <sub>3</sub>	1586	216		55.7	883	NH <sub>3</sub>			36	1-2	2*	H302
Oxalic Acid	1,900	95.5*		97.8	1857	Formic Acid		11.4	125-175	1-5	2*	H302+H312, H318, H402
Oxalic Acid	1,900	95.5*		97.8	1857	H <sub>2</sub> (via formic acid)		42.9	25-120 (cat.)	3-Inf		H302+H312, H318, H402
Oxalic Acid · 2H <sub>2</sub> O	1,653	139.0*		69.8	1154	Oxalic Acid (drying)			100	3-Inf		H302+H312, H318, H402
Methanol	729	Miscible	137.4% (equivalent because it does not include oxygen)	1088		H <sub>2</sub>		-49.3	200-300	7	2-3	H225, H301, H311, H331, H370
Formic acid												H226, H302, H331, H314, H318, H402
Sodium formate	1220	Miscible	95.60%	1152	H <sub>2</sub>		32		200-350	5	2	
	1920	972*	64.70%	1229		H <sub>2</sub>		-89.8	Ambient	5	1	H315, H319, H335
						(aqueous)						

\* at 27.8°C

+ at 20.0°C

‡ based on aqueous sodium compounds and solid calcium compounds

\* based on aqueous potassium compounds and solid calcium compounds

‡ when using pure CO<sub>2</sub> as feedstock

currently commercially pursued by companies like Carbon Engineering who adopted this process from the pulp and paper industry (Kraft process).<sup>20</sup> If Na<sub>2</sub>CO<sub>3</sub> is produced from an aqueous solution, it is likely that hydrated and bicarbonate species form.<sup>52</sup> Sodium carbonate is known to form monohydrate, heptahydrate and decahydrate. The co-crystallization of water substantially reduces CO<sub>2</sub> mass fraction and CO<sub>2</sub>-density, which are 15.4 CO<sub>2</sub> wt% and 225 kg m<sup>-3</sup> for the decahydrate (other hydrates are listed in Table 2). Due to the higher water content, hydrated forms of Na<sub>2</sub>CO<sub>3</sub> are expected to have longer shelf lives. Sodium bicarbonate is an interesting by-product with a density of 2200 kg m<sup>-3</sup> and CO<sub>2</sub> mass fraction that is higher than that of Na<sub>2</sub>CO<sub>3</sub> (52.4 CO<sub>2</sub> wt% if all CO<sub>2</sub> is removed from sodium, *e.g.* using Ca(OH)<sub>2</sub> to form

CaCO<sub>3</sub> which then can be thermally decomposed to obtain CO<sub>2</sub>). However, when considering the energetically attractive low temperature thermal decomposition of NaHCO<sub>3</sub> to Na<sub>2</sub>CO<sub>3</sub> at 100–200 °C, only 50% of the CO<sub>2</sub> is released leading to an effective CO<sub>2</sub> mass fraction of 26.2 CO<sub>2</sub> wt% and a CO<sub>2</sub>-density of 576 kg m<sup>-3</sup>. The preparation of NaHCO<sub>3</sub> is relatively simple as it can be precipitated by bubbling CO<sub>2</sub> through aqueous NaCO<sub>3</sub> brines/solutions. This way of producing NaHCO<sub>3</sub> has become a significant industrial process in the US as part of Na<sub>2</sub>CO<sub>3</sub> production from Trona.<sup>53</sup>

Potassium carbonate is the last alkali metal carbonate we consider, as rubidium and caesium are too costly. Anhydrous K<sub>2</sub>CO<sub>3</sub> has a density of 2430 kg m<sup>-3</sup>, and due to the heavier metal cation, a relatively low CO<sub>2</sub> mass fraction of 31.8 CO<sub>2</sub> wt%,





and a CO<sub>2</sub>-density of 774 kg m<sup>-3</sup>. Similar to Na<sub>2</sub>CO<sub>3</sub>, K<sub>2</sub>CO<sub>3</sub> does not decompose to CO<sub>2</sub> and K<sub>2</sub>O upon heating, which is an extremely endothermic reaction with a reaction enthalpy of 393.5 kJ mol<sup>-1</sup>. Thus, K<sub>2</sub>CO<sub>3</sub> is thermally extremely stable; however, it is very hygroscopic and dissolves 1103 g L<sup>-1</sup>. This strong hygroscopicity typically limits its shelf life to about 1–5 years depending on the storage conditions. The regeneration of K<sub>2</sub>CO<sub>3</sub> can be accomplished in a similar manner to Na<sub>2</sub>CO<sub>3</sub> by using Ca(OH)<sub>2</sub> to form KOH and CaCO<sub>3</sub> which is a mildly exothermic process and likely to be exergonic at ambient conditions. When K<sub>2</sub>CO<sub>3</sub> is produced in aqueous solutions or directly from KOH, the formation of sesquihydrate is possible (K<sub>2</sub>CO<sub>3</sub>·3/2H<sub>2</sub>O) which reduces the CO<sub>2</sub> mass fraction to 26.6 CO<sub>2</sub> wt% and the CO<sub>2</sub>-density to 645 kg m<sup>-3</sup>. To obtain the anhydrous form and drive off the water, the sesquihydrate can be dried at 200–350 °C. The reaction of gaseous CO<sub>2</sub> with aqueous KOH to obtain pure K<sub>2</sub>CO<sub>3</sub> is a commercial process whereby the K<sub>2</sub>CO<sub>3</sub>·3/2H<sub>2</sub>O is separated *via* crystallization under vacuum with cooling and subsequently dried to achieve a purity of 98–100%.<sup>54</sup> In some industrial K<sub>2</sub>CO<sub>3</sub> production processes, KHCO<sub>3</sub> is obtained as a precursor.<sup>54</sup> For KHCO<sub>3</sub>, two CO<sub>2</sub> regeneration routes exist. If KHCO<sub>3</sub> is converted to K<sub>2</sub>CO<sub>3</sub> at around 100–120 °C, the effective CO<sub>2</sub> mass fraction of the CO<sub>2</sub> storage medium is 22.0 CO<sub>2</sub> wt% and the CO<sub>2</sub>-density is 477 kg m<sup>-3</sup>. If complete CO<sub>2</sub> recovery is considered, *i.e.* with Ca(OH)<sub>2</sub>, the effective CO<sub>2</sub> mass fraction of the CO<sub>2</sub> storage medium is 44.0 CO<sub>2</sub> wt% and the CO<sub>2</sub>-density is 954 kg m<sup>-3</sup>.

### Alkaline earth metal carbonates

Magnesium carbonate is the lightest alkaline earth metal discussed here and has a density of 2958 kg m<sup>-3</sup>. With a CO<sub>2</sub> mass fraction of 52.2 CO<sub>2</sub> wt%, this results in an effective CO<sub>2</sub> storage density of 1544 kg m<sup>-3</sup>. The solubility of MgCO<sub>3</sub> is low with only 0.1 g L<sup>-1</sup>, which is certainly an advantage when producing MgCO<sub>3</sub> from aqueous solutions. In aqueous solutions MgCO<sub>3</sub> can be produced *via* the reaction with aqueous NaHCO<sub>3</sub>; however, if reacted with Na<sub>2</sub>CO<sub>3</sub>, basic MgCO<sub>3</sub> is formed (a hydrated complex of MgCO<sub>3</sub> and Mg(OH)<sub>2</sub>). In the presence of water, MgCO<sub>3</sub> may form dihydrate, trihydrate and pentahydrate crystals which have significantly lower CO<sub>2</sub>-densities as seen in Table 2. To reduce the water content, drying at temperatures above 157 °C is necessary but drying is not complete until a temperature of 300 °C is reached.<sup>55</sup> Alternatively, the anhydrous salt can be produced from a Mg(OH)<sub>2</sub> slurry directly if high CO<sub>2</sub> partial pressures are available (0.4–0.5 MPa), which is the preferred industrial process for high purity MgCO<sub>3</sub> production. This pathway includes the formation of aqueous bicarbonate under moderate temperatures and pressures before being vacuum dried. Magnesium bicarbonate is not a stable side-product, only exists in aqueous solution, and decomposes into CO<sub>2</sub> and H<sub>2</sub>O during drying while forming MgCO<sub>3</sub>.<sup>56</sup> The regeneration of the magnesium carrier and release of CO<sub>2</sub> can be achieved by thermal decomposition over a temperature range of 360–800 °C (800 °C are needed for complete conversion).<sup>56</sup> In the industrial calcination process for the production of MgO from MgCO<sub>3</sub> minerals,

temperatures between 700–2000 °C are used. However, lower calcination temperatures of 540–800 °C lead to more reactive MgO which is more suitable for CO<sub>2</sub> adsorption.<sup>57</sup> The reaction enthalpy with 116.9 kJ mol<sup>-1</sup> is relatively low and presents an interesting “low energy” pathway for CO<sub>2</sub> storage compared to some of the other carbonate carriers. Other regeneration routes include acid treatment with HCl or H<sub>2</sub>SO<sub>4</sub>. A recent review offers insights into several modifications to MgO that can improve its use as an adsorbent for CO<sub>2</sub>, including the use of promoters, hybrid materials, and amine functionalization; however, benefits such as cyclic stability are more relevant for CO<sub>2</sub> capture.<sup>58</sup>

Calcium carbonate has a higher molecular weight than MgCO<sub>3</sub>. While the density of CaCO<sub>3</sub> is similar to MgCO<sub>3</sub>, the higher mass of calcium leads to a lower CO<sub>2</sub> mass fraction and CO<sub>2</sub>-density with 44.0 CO<sub>2</sub> wt% and 1244 kg m<sup>-3</sup> respectively. Calcium carbonate is highly insoluble, only 0.013 g dissolve in 1 L of water at 25 °C. Furthermore, CaCO<sub>3</sub> does not form hydrates even in aqueous solutions. A monohydrate of CaCO<sub>3</sub> exists but does not form under normal circumstances (forms *via* a Mg-rich amorphous calcium carbonate precursor)<sup>59</sup> and the hexahydrate is only stable below 7 °C.<sup>60</sup> Calcium carbonate is an intermediate product in DAC systems where aqueous NaOH is used to capture the CO<sub>2</sub> followed by the reaction of solid Ca(OH)<sub>2</sub> with aqueous Na<sub>2</sub>CO<sub>3</sub> to form solid CaCO<sub>3</sub>.<sup>51</sup> Calcium carbonate is easy to separate from the NaOH solution due to its low solubility and lack of bicarbonate and hydrate side reactions. Thus, when heating CaCO<sub>3</sub> all energy goes towards the actual regeneration of CaCO<sub>3</sub> and not into reversing side reactions. The regeneration of CaCO<sub>3</sub> occurs at temperatures greater than 650 °C (industrial quicklime processes use >900 °C to achieve appreciable reaction rates)<sup>61,62</sup> and the reaction enthalpy of the reaction is 178.4 kJ mol<sup>-1</sup>. This is substantially higher than the reaction enthalpy of MgCO<sub>3</sub> and one might wonder why DAC systems use Ca instead of Mg. Besides the higher solubility of MgCO<sub>3</sub> and formation of hydrates (drying hydrates would increase energy demand), Mg(OH)<sub>2</sub> is weaker than Ca(OH)<sub>2</sub> and the reaction of Mg(OH)<sub>2</sub> with aqueous Na<sub>2</sub>CO<sub>3</sub> is endergonic ( $\Delta G_{\text{Mg}} = 34.8 \text{ kJ mol}^{-1}$  *vs.*  $\Delta G_{\text{Ca}} = -18.4 \text{ kJ mol}^{-1}$ ) and would not happen spontaneously at ambient conditions.

### Other solids

Oxalic acid is a commercially available solid dicarboxylic acid with the formula H<sub>2</sub>C<sub>2</sub>O<sub>4</sub>. Oxalic acid has a density of 1900 kg m<sup>-3</sup> and an extremely high CO<sub>2</sub> mass fraction of 97.8 CO<sub>2</sub> wt% leading to a remarkably high CO<sub>2</sub>-density of 1857 kg m<sup>-3</sup>. In aqueous solution H<sub>2</sub>C<sub>2</sub>O<sub>4</sub> may form a dihydrate crystal which can be reduced to its anhydrous form by drying at modest temperatures of 100 °C.<sup>63</sup> These properties make it a very interesting compound for CO<sub>2</sub> transport and storage.

While there are other carboxylic acids, such as citric acid that are interesting from a CO<sub>2</sub> storage perspective, the challenge is to find reaction pathways for the production of these chemicals using CO<sub>2</sub>. At the same time a viable CO<sub>2</sub> regeneration pathway is



necessary to recover and reuse the carrier if a non-ubiquitous reactant is used as carrier. Oxalic acid is a compound that possesses both of these characteristics. Traditionally,  $\text{H}_2\text{C}_2\text{O}_4$  is produced from carbohydrates using nitric acid, a process which was discovered in 1776. Nevertheless, commercial processes for a  $\text{CO}_2$ -based synthesis exist *via* the reverse water gas shift reaction, the dialkyl oxalate process and traditional acidification; however, recently new  $\text{CO}_2$ -based reaction pathways have been discovered. Oxalate can be produced directly from  $\text{CO}_2$  *via* electrochemical routes using aprotic solvents with faradaic efficiencies up to 80%.<sup>64</sup> Alternatively, oxalate can be produced from CO (*e.g.* from  $\text{CO}_2$  electrolysis), biomass or the coupling of formate (which can be produced from CO or  $\text{CO}_2$ ). The oxalate can then be converted to  $\text{H}_2\text{C}_2\text{O}_4$  *via* traditional acidification or electrodialysis.<sup>65</sup> When  $\text{H}_2\text{C}_2\text{O}_4$  is heated to about 125–175 °C it decomposes to  $\text{CO}_2$  and formic acid ( $\Delta H = 11.4 \text{ kJ mol}^{-1}$ ).<sup>66</sup> Formic acid can be further decomposed to  $\text{CO}_2$  and  $\text{H}_2$  at ambient temperatures using catalysts ( $\Delta H = 42.9 \text{ kJ mol}^{-1}$ ) as described in the following sections.<sup>67</sup> Oxalic acid is already a  $\text{C}_2$  molecule and can become a new base chemical for polymers, enabling numerous new  $\text{CO}_2$  utilization pathways that offer long term storage.<sup>65</sup>

### Down-selection of solids

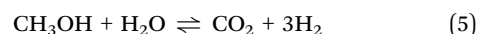
Among the various solids evaluated,  $\text{NaHCO}_3$ ,  $\text{MgCO}_3$ ,  $\text{CaCO}_3$  and  $\text{H}_2\text{C}_2\text{O}_4$  stand out as potentially attractive  $\text{CO}_2$  storage media. They are stable at ambient conditions and exhibit some of the highest  $\text{CO}_2$  mass fractions and  $\text{CO}_2$ -densities. If a concentrated  $\text{CO}_2$  stream is available  $\text{NaHCO}_3$  is relatively easy to precipitate in aqueous NaOH solutions without any hydrate by-products. For regeneration,  $\text{NaHCO}_3$  can be integrated with current DAC systems that rely on a  $\text{NaOH}$ – $\text{Ca}(\text{OH})_2$  cycle. If DAC systems run 100% on renewables like wind and solar, this external source of  $\text{NaHCO}_3$  can be added to bridge intermitencies and increase the overall capacity factor of the DAC systems while improving the economies of scale. Similarly,  $\text{CaCO}_3$  can be used in combination with DAC systems. Calcium carbonate has the advantage that it can be used with lower  $\text{CO}_2$  partial pressures and NaOH. Magnesium carbonate is really attractive due to its low regeneration energy requirement and might be an interesting alternative if high  $\text{CO}_2$  partial pressures are available. One of the most exciting  $\text{CO}_2$  storage chemicals is  $\text{H}_2\text{C}_2\text{O}_4$  due to its extremely high  $\text{CO}_2$  mass fraction, extremely high  $\text{CO}_2$ -density as well as its chemistry. The  $\text{CO}_2$ -density of  $\text{H}_2\text{C}_2\text{O}_4$  exceeds the density of liquid  $\text{CO}_2$ ; however, it is important to understand that in powder form this density is likely to decrease by approximately 50%. Nevertheless, even in powder form its density is still very attractive for transportation and storage applications.

### Liquid organic carbon dioxide carriers

Liquid organic carriers with high carbon contents are discussed in this section and properties are included in Table 2. Urea was reviewed but does not show promise as a candidate. Additional details on urea are provided in the ESI.†

### Methanol

Methanol stores CO rather than  $\text{CO}_2$ , and would require additional oxygen if it was necessary to produce  $\text{CO}_2$  upon decommissioning  $\text{CO}_2$  storage systems. Methanol, which has a  $\text{H}_2$  content of 12.5  $\text{H}_2$  wt% (99  $\text{kg m}^{-3}$ ), can be stored as a liquid at ambient conditions, and offers a CO content of 87.4  $\text{CO}_2$  wt% (which for the sake of comparison can be translated into 137.4  $\text{CO}_2$  wt% and 1088  $\text{kg m}^{-3}$ ). Storing  $\text{CO}_2$  *via* methanol has been demonstrated commercially *via* different pathways, such as direct catalytic conversion using  $\text{H}_2$ , conversion *via* hydrides, and integration of amine-captured  $\text{CO}_2$  or biomass conversion.<sup>68–70</sup> Recently methanol production using  $\text{CO}_2$  and green  $\text{H}_2$  has been demonstrated by Carbon Recycling International, making it one of the most mature liquid carriers for both  $\text{CO}_2$  and  $\text{H}_2$ .<sup>71</sup> Recent reviews highlight the ways in which techniques such as photochemical, electrochemical,<sup>72</sup> and biological processes can increase the rate, efficiency, and selectivity of conversion.<sup>73</sup> For methanol or other alcohols,  $\text{CO}_2$  can be recovered during the decommissioning of a storage facility, or upon delivery, in a controlled manner.<sup>74</sup> For example, steam reforming for dehydrogenation under elevated pressures (2 MPa) and temperatures (250–250 °C) has been widely investigated (eqn (5)).<sup>75</sup> As evident in the reaction, the fixation process for methanol forms  $\text{H}_2\text{O}$  as a by-product, and its regeneration process requires  $\text{H}_2\text{O}$ . Dehydrogenation temperatures vary widely in literature and have been reported as high as 450 °C in commercial systems.<sup>76</sup>

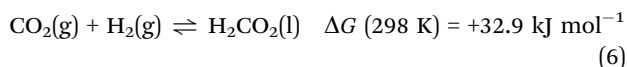


### Formic acid and formate salts

Formic acid and formate salts are stable  $\text{H}_2$  carriers that can be used to store and transport CO and  $\text{CO}_2$ . Formic acid has a high  $\text{CO}_2$  capacity (95.6  $\text{CO}_2$  wt% and 1152  $\text{kg m}^{-3}$ ) and low  $\text{H}_2$  capacity (4.4  $\text{H}_2$  wt% and 53  $\text{kg m}^{-3}$ ). It is already stored and transported in bulk quantities for a number of industrial uses, particularly in Europe, and tends to be transported in a non-pure form to eliminate issues relating to venting and flammability. With proper storage, formic acid can have a shelf life of two years or more.<sup>77</sup> The potential safety and stability of formic acid is highlighted by companies such as OCOchem that are developing catalytic approaches for converting  $\text{CO}_2$  to products under mild conditions.<sup>76</sup> Formate salts ( $\text{HCOOM}$ ;  $\text{M} = \text{Li}^+$ ,  $\text{Na}^+$ ,  $\text{K}^+$ ,  $\text{Cs}^+$ ,  $\text{NH}_4^+$ ) use a formate bicarbonate cycle for storage.<sup>78</sup> Formate salts will have different features depending on the cation, as noted in Table 2. For example, when the cation is sodium,  $\text{CO}_2$  capacity is 64.7  $\text{CO}_2$  wt% with  $\text{CO}_2$ -density of 1229  $\text{kg m}^{-3}$  in comparison to when the cation is potassium and the  $\text{CO}_2$  capacity is 52.3  $\text{CO}_2$  wt% with  $\text{CO}_2$ -density of 994  $\text{kg m}^{-3}$ . The direct hydrogenation of  $\text{CO}_2$  into FA or FS is challenging due to the unfavorable phase change (eqn (6)), but the thermodynamic preference can be altered when the reaction is carried out in aqueous forms, with  $\Delta G$  of  $-4 \text{ kJ mol}^{-1}$ .<sup>79</sup> There are multiple pathways of storing CO or  $\text{CO}_2$  in the form of FA or FS other than direct hydrogenation (*e.g.* *via* methanol),



but commercialization requires improvements to selectivity, product separations and stability. As noted in a recent review by Duarah *et al.*, emerging electro-chemical pathways have been developed to improve these processes under ambient conditions, with faradaic efficiencies achieved above 90%.<sup>80</sup> One advantage of FA and FS is that they can be dehydrogenated under mild conditions or used directly upon decommissioning of a storage facility to manufacture a wide range of chemicals.<sup>81</sup>



### Down-selection of LOHC

Among the liquid carriers that can simultaneously store  $\text{CO}_2$  and  $\text{H}_2$ , methanol and FA are the most promising as they have relatively high technology maturities and favourable gravimetric and volumetric  $\text{CO}_2$  densities. Synthesis of FS has largely been demonstrated for CO and not  $\text{CO}_2$ , and justifies us not evaluating it further in the following analysis. The shelf life of these liquid carriers may be a few years even if stored properly, which is short compared with most of the solid carriers listed in Table 2 and may make them more viable for transportation applications. Additionally, unlike sorbents and solid carriers, LOHC require a deformation of  $\text{CO}_2$ , which requires substantial amounts of energy. We decided to include these materials in our analysis as there have been major advancements in reactor design as well as direct electroreduction of  $\text{CO}_2$  focused on lowering the cost of  $\text{CO}_2$  utilization,<sup>82,83</sup> which will also lower the cost of LOHC for  $\text{CO}_2$  storage. For example, Sun *et al.* review the promise of tuning two-dimensional nanosheets to avoiding the use of catalysts based on costly noble metals.<sup>84</sup> Moving towards an electrochemical approach may improve overall synergies with DAC facilities with dedicated renewables or established grid connections.

### Storage analysis

The importance of gravimetric capacity becomes apparent when estimating the quantity of material required to store the same amount of  $\text{CO}_2$  (Fig. 4). Oxalic acid and FA require very little material per unit of  $\text{CO}_2$  stored, while  $\text{NaHCO}_3$ , when removing 0.5  $\text{CO}_2$  per Na, requires substantial amounts of material. Methanol technically only stores CO, so an additional amount of oxygen is required to provide  $\text{CO}_2$ . Volumetric capacity and the phase of the material and flammability of material are key variables influencing the physical footprint of the system. At the pilot scale, FA and methanol have the largest footprint per unit of  $\text{CO}_2$  stored due to the space required for safety, despite their good gravimetric capacities. NFPA 30 requires spatial separation of large-scale storage of Class 1 flammable liquids of at least 15 meters, and we conservatively use this value to estimate safety spacing for methanol and formic acid. Liquid  $\text{CO}_2$  has the smallest footprint due to its high density and relatively small assumed safety spacing requirement. It offers high densities, but requires thermal insulation and liquefaction has a high energy consumption. Liquified  $\text{CO}_2$  is energetically costly and subject to boil-off issues, making it unsuitable for long-term  $\text{CO}_2$  storage.

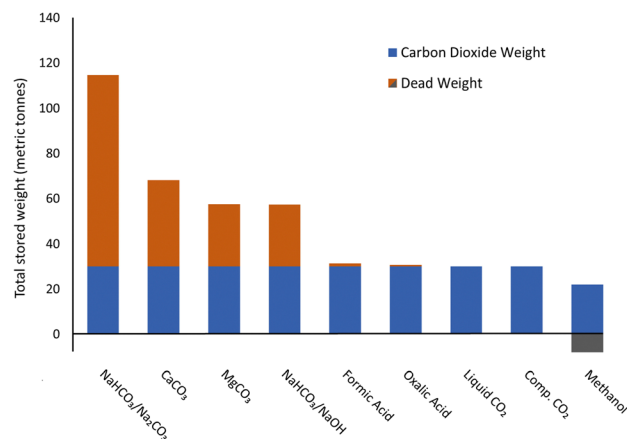


Fig. 4 Quantity of carrier weight required to store 30 t $\text{CO}_2$ . Carbon dioxide weight is excluded for methanol as it stores CO rather than  $\text{CO}_2$ .

Results are substantially different at the regional hub scale (Fig. 5), as liquid  $\text{CO}_2$  tanks do not achieve great economies of scale (110  $\text{m}^3$  compared to 28  $\text{m}^3$  capacity for the pilot facility) relative to other materials. The poor gravimetric capacity of  $\text{NaHCO}_3$  does not outweigh the great economies of scale achieved with bulk powder silos, and it has a similar footprint intensity as liquid  $\text{CO}_2$ . Flammable liquid storage also scales well with capacity, and methanol and FA require less than 60 storage vessels, compared with the bulk powder materials that require between 100–400, and liquid  $\text{CO}_2$  which requires nearly 8260 tanks. Oxalic acid, which offers the smallest land footprint for a regional hub, would still require a space the size of approximately 22 soccer fields (7140  $\text{m}^2$ ) or 6.5% of an

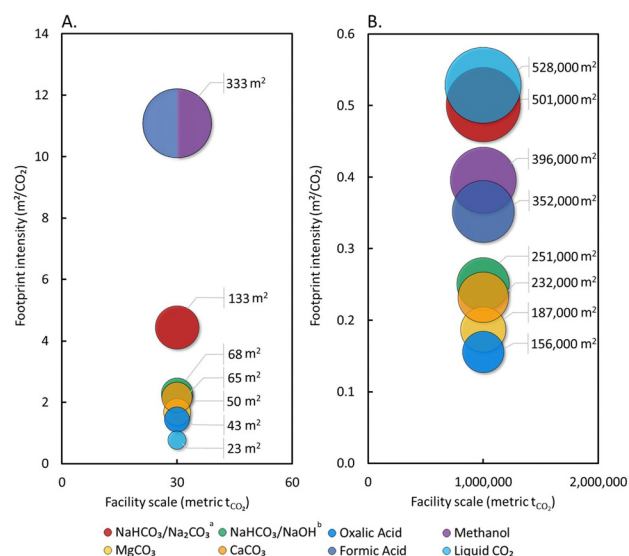


Fig. 5 Land footprint intensity per tonne of  $\text{CO}_2$  stored and total physical footprint required to store  $\text{CO}_2$  for the following scenarios: (A) pilot facility (three years of storage, or 30 t $\text{CO}_2$ ) and (B) regional hub (one year of storage or 1 Mt $\text{CO}_2$ ). The area of circle represents the total land footprint required ( $\text{m}^2$ ). For reference, a soccer field is 7140  $\text{m}^2$  and an average United States landfill is 2.4 million  $\text{m}^2$ . Assumes 50% powder void fraction. <sup>a</sup>Removing 0.5  $\text{CO}_2$  per Na. <sup>b</sup>Removing 1.0  $\text{CO}_2$  per Na.

average landfill in the United States. Carbonate salts require slightly more land area at the regional hub scale than oxalic acid (20–61% more), but still perform far better than methanol and FA at all scales studied.

### Transportation analysis

Considering B-train trucks, we find that the quantity of CO<sub>2</sub> that can be transported per vehicle is limited by weight, except for sorbents where the volume of the tanks limited CO<sub>2</sub> delivery per truck (Table S2, ESI†). Methanol, formic acid, and oxalic acid can deliver more CO<sub>2</sub> per truck than liquified CO<sub>2</sub> trucks, and all return empty except for oxalic acid which has very little dead weight. Liquid chemical carriers tend to outperform solid carriers due to their high carbon contents and good bulk densities. It is notable that for methanol, the mass of CO<sub>2</sub> transported per tonne of methanol is 1.38 tonne, which is higher than the mass of the methanol required. This is due to the fact that additional oxygen (when reforming in the form of steam) is required when releasing CO<sub>2</sub> from methanol. Oxalic acid has an extremely high gravimetric capacity of 97.8 CO<sub>2</sub> wt%, which leads to similar transport characteristics as liquefied CO<sub>2</sub>. In comparison, the weight of the returning trucks for other carbonate salts, can be almost as heavy as a full truck which increases energy requirement of CO<sub>2</sub> transport. MOFs do not have as significant a deadweight, but are limited in volume as it relies on compressing gaseous CO<sub>2</sub>.

Moving 1 million tonnes of CO<sub>2</sub> from a hypothetical plant annually through methanol, formic acid, oxalic acid, and liquid CO<sub>2</sub> would require operating 39–56 B-trains each day. Moving the same amount of CO<sub>2</sub> *via* MOF or future MOF would need

114 or 71 B-trains daily, respectively. Moving CO<sub>2</sub> with other solids can require up to 207 B-trains daily due to limited capacity. Just comparing across a single round-trip, methanol can deliver the most CO<sub>2</sub>, with only 39 trucks required to move daily CO<sub>2</sub> production in the regional hub scenario. No truck transportation technology can match the low transportation energy of supercritical pipelines.

Energy consumption per truck is a function of weight and increases linearly with round-trip distance (31–40 MJ per km-truck). The total transport energy for trucking shown in Fig. 6 accounts for diesel fuel consumed by a truck fleet moving 1 million tonnes of CO<sub>2</sub>. Methanol, formic acid, and oxalic acid can deliver CO<sub>2</sub> with diesel consumption close to or less than trucking liquified CO<sub>2</sub>. Emissions associated with diesel consumption derived using our approach were between 45 and 57 grams of CO<sub>2</sub> equivalents per tonne-km, which aligns well with emission factors reported for long-haul trucks (57 gCO<sub>2</sub> per t-km).<sup>85</sup> Emissions associated with diesel consumption and with recompression for pipelines will have a negligible impact, especially over expected transportation distances (<500 km). The emissions breakeven distance shows that pipeline is the most efficient mode of CO<sub>2</sub> transport, followed by methanol, formic acid, oxalic acid, liquid CO<sub>2</sub> and future MOF trucking. Lowering the speed of trucks from 100 to 80 kg h<sup>-1</sup> reduces the transport energy intensity by 15–20% while increasing the breakeven distance by 19–23% in all carriers considered. Smaller changes were observed for solid carriers due to the heavy weight of the returning trucks. However, the relative orders amongst carriers in terms of energy intensity and breakeven distances are unaffected. The breakeven distance of methanol, the best-performing carrier,

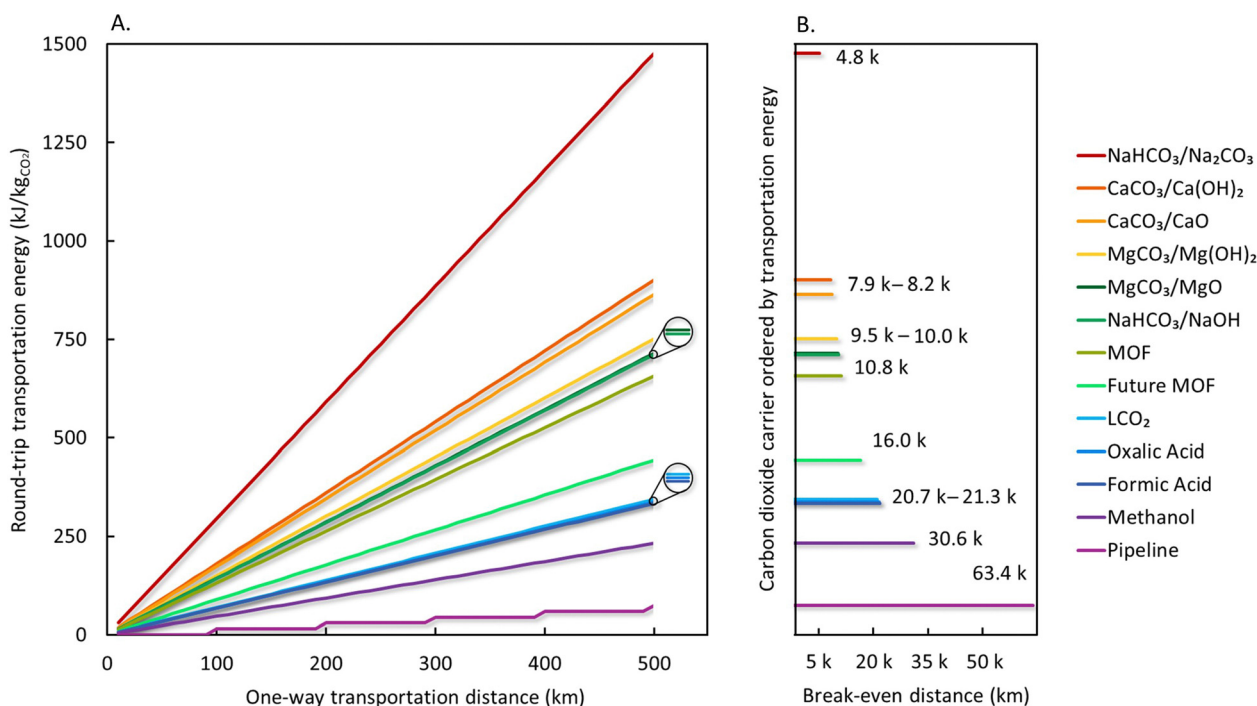


Fig. 6 Truck driving distances and (A) estimated energy consumed for transport of CO<sub>2</sub> by way of gas, liquid, and solid carriers, and (B) break-even distance before more CO<sub>2</sub> is emitted during transportation than is stored. Values are presented in Table S2 (ESI†).





is 37.8 km when operating trucks at  $80 \text{ km h}^{-1}$ , which is still considerably shorter than 63.4 km of  $\text{CO}_2$  pipeline. Trucking  $\text{CO}_2$  with MOF will create more emissions during delivery compared to conventional means even when its uptake capacity can be increased in the future. This is due to the dead weight and volume occupied by MOF pellets limiting the quantity of the transported  $\text{CO}_2$ . The quantity of  $\text{CO}_2$  transported using a truck filled with MOFs can be further increased by lowering temperature or increasing pressure during transport, but these strategies were not considered in this analysis due to the lack of data.

Pathways for capturing  $\text{CO}_2$ , converting it for storage, loading and unloading a vehicle, and recovering the  $\text{CO}_2$  have very different processes involved, and estimating energy consumption is outside the scope of this analysis. For example, the relatively low diesel consumption required for methanol and FA transport is likely to be overshadowed by the energy intensive processes required for hydrogenation and dehydrogenation, unless these processes can rely on low-carbon electricity. There are concepts to take advantage of high decarbonation temperatures in thermal energy storage, *e.g.* in thermal solar plants,<sup>86</sup> which might present an interesting integration of systems that improves life-cycle performance. Upfront compression requirements for sorbent transportation technologies at the scale of a refuelling station must be compared with relevant scale systems for liquified  $\text{CO}_2$  or supercritical pipeline  $\text{CO}_2$ , as the behaviour of  $\text{CO}_2$  varies substantially from ideal in these ranges.<sup>35,87,88</sup> Whether liquid carriers outcompete sorbents or solid carriers on a carbon emission or energy intensity basis will need to be assessed through life-cycle assessment that determines impacts from  $\text{CO}_2$  transportation and from  $\text{H}_2$  transportation.

## Concluding remarks

In this analysis, we reviewed several classes of materials for their viability as storage materials for  $\text{CO}_2$ . Material classes were identified based on carbonate chemistry in nature and industry, consideration in  $\text{CO}_2$  capture systems, and consideration for  $\text{H}_2$  storage. Materials were screened based on their ability to offer stable but reversible storage over relevant time scales, their theoretical gravimetric and volumetric storage capacities, compatibility with existing solid, liquid, and gaseous infrastructure currently used in industry, and availability of experimental data describing performance. The quantity of material and subsequent number of trucks and storage units were estimated for storage capacities of 30 t $\text{CO}_2$  and 1 Mt $\text{CO}_2$  and capture rates of 10 tpy and 1 Mtpy.

While many materials derived from  $\text{CO}_2$  have been ruled out as options for permanent sequestration of  $\text{CO}_2$  due to limited compound stability under ambient storage conditions, the concept of temporary storage in the form of an environmentally friendly cheap compound to bridge temporal, spatial and economic scale gaps may not be that absurd. This is especially true considering the dramatically poor scaling of liquid  $\text{CO}_2$

stationary storage compared with solid chemical carriers (Fig. 5). Our first-order evaluation of materials for  $\text{CO}_2$  storage and transportation suggests that the land footprint and number of trucks required to manage  $\text{CO}_2$  in the absence of geologic storage and pipelines is large, but improved over gaseous and liquified  $\text{CO}_2$  storage. We also find that the greenhouse gas emissions associated with transporting  $\text{CO}_2$  by diesel truck is negligible but still greater than emissions associated with recompression in pipelines. Both  $\text{CO}_2$  pipelines and liquefaction facilities are capital-intensive infrastructure to build, especially at small annual capacities, and would require  $\text{CO}_2$  sources and sinks to remain relatively fixed. Other storage and transport options – such as chemicals and sorbents – may offer flexibility to emerging distributed and highly mobile  $\text{CO}_2$  capture technologies that are positioned to tackle our climate crisis.

Carbonates are possible candidates for stationary storage but it is unclear whether the long shelf life of the material will offset challenges associated with acquiring the large initial quantity of carrier material required (Fig. 4). Formic acid, oxalic acid, and methanol provide higher densities than cryogenic liquid  $\text{CO}_2$ , with less starting material required than carbonates. Tradeoffs between material requirements (Fig. 4), land requirements (Fig. 5), storage duration (Table 2) and energy consumption (Fig. 6) will all influence cost. While it is not within the scope of this study to estimate which method may be most economic for long duration  $\text{CO}_2$  storage, we offer the following thoughts on cost. First, the maturity, long storage duration, and high density of carbonates could lead to low costs. Second, the ultra-high storage capacity of oxalic acid, along with the potential to be readily produced from  $\text{CO}_2$  and water under mild conditions could also lead to low costs. The same is true for formic acid, and both acids have gained increased attention as valuable products of electroreduction of  $\text{CO}_2$  at  $\sim 400 \text{ \$ per t}$  market value.<sup>89</sup> Third, the cost of LOHC that require hydrogen will be highly dependent on the price of  $\text{H}_2$ . Fourth, for some of our top candidates, we wish to highlight an exciting benefit, which would be the direct capture of  $\text{CO}_2$  into liquid or solid materials for storage without the need for  $\text{CO}_2$  compression, examples of which are noted by Gutierrez-Sanchez *et al.* for formic acid and methanol.<sup>90</sup> Future experimental and engineering design work are needed to advance the integration of storage materials into  $\text{CO}_2$ -capture concepts, and we hope this study will draw attention to this research gap.

Finally, we identify multiple pathways for low-energy recovery of  $\text{CO}_2$  from storage materials. This is important for recycling solid and liquid carrier materials for reuse or sale. In a circular economy there will be many different  $\text{CO}_2$ -sources and technologies utilized to control  $\text{CO}_2$  emissions. Thus, it is likely that various  $\text{CO}_2$  storage media will find use in a circular economy upon decommissioning the  $\text{CO}_2$  storage system.<sup>91</sup> At the same time, given the scale of storage required, it is essential to find alternatives to materials with high supply risk and cost. The issue of material criticality for clean energy systems has led to national investments in domestic production of materials such as lithium. It is notable that our top



candidates for storage do not rely on critical materials, however, we do note that sorbents may require cobalt, nickel, or manganese, and that some catalysts for LOHC use critical materials such as iridium. Considering the potential market growth of liquid H<sub>2</sub> carriers<sup>92,93</sup> with careful planning and road mapping, integrating H<sub>2</sub> and CO<sub>2</sub> transportation may likely have economic and environmental benefits.<sup>10</sup> We envision scenarios where large potential off-takers of CO<sub>2</sub>, such as the cement industry, use H<sub>2</sub> to provide clean heat and electricity.

The ability to recycle solid sorbent materials such as MOFs is unknown, and their use may be limited to CO<sub>2</sub> capture and transportation applications where they will undergo frequent cycling. While the projected future cost of MOFs for H<sub>2</sub> and natural gas storage ranges between \$10–71 per kg-sorbent,<sup>94</sup> some of the best performing MOFs for CO<sub>2</sub> are unlikely to achieve such low costs. In comparison, activated carbon sells on markets such as Alibaba at as low as \$0.45–6 per kg-sorbent. As such, the use of MOFs for small stationary storage, or short duration storage with high cycling, such as for transportation, is more feasible than large-scale bulk storage. It is important to note that our sorbent-based transportation analysis was limited by the lack of high-pressure CO<sub>2</sub> adsorption data points; further measurement of MOFs, activated carbons, and zeolites at high-pressure environment relevant to CO<sub>2</sub> storage would reduce the technical uncertainty of sorbent-based storage and transportation.

In conclusion, material emplacement of CO<sub>2</sub>, or material-based storage at large scales, should be taken seriously as a CO<sub>2</sub> storage solution as it can be: (1) deployed today; (2) geographically agnostic; (3) used as a form of bulk CO<sub>2</sub> transportation, avoiding the construction of pipelines; and (4) decommissioned and monitored. Carbon dioxide storage and transportation are essential components of CO<sub>2</sub> removal, and the discovery and development of advanced storage technologies could play a critical role in enabling the deployment of capture technologies in the next decade. As summarized in this study, the benefits and challenges of each material reviewed are highly specific, and will require further analysis to verify storage durability and to identify the most cost-effective solutions. We encourage the community of scientists advancing the use of materials for CO<sub>2</sub> capture and for utilization to apply their knowledge to this pressing application.

## Author contributions

H. B. conceptualized and conceived the analysis. H. B., T. L., and F. R. developed the methodology. All authors conducted the investigation, curated the data, wrote the original draft, and reviewed and edited the paper. H. B., F. R., and T. L. visualized the results. H. B. supervised and obtained funding and resources for the project.

## Conflicts of interest

There are no conflicts to declare.

## Acknowledgements

The authors gratefully acknowledge support from the Laboratory-Directed Research and Development program at Lawrence Berkeley National Laboratory (LBNL), and funding from the U.S. Department of Energy Office of Basic Energy Sciences, under Contract Number DE-AC02-05CH11231 with LBNL. The views and opinions of the authors expressed herein do not necessarily state or reflect those of the United States Government or any agency thereof. Neither the United States Government nor any agency thereof, nor any of their employees, makes any warranty, expressed or implied, or assumes any legal liability or responsibility for the accuracy, completeness, or usefulness of any information, apparatus, product, or process disclosed, or represents that its use would not infringe privately owned rights. We gratefully thank the two reviewers, Hiroyasu Furukawa for his insights on metal organic framework performance, and Damien Jullié for his constructive review that led to the development of Fig. 1.

## References

- 1 E. Rubin and H. De Coninck, IPCC special report on carbon dioxide capture and storage, *TNO Cost Curves CO<sub>2</sub> Storage, Part 2*, UK Cambridge Univ. Press, 2005.
- 2 S. D. Supekar, T. H. Lim and S. J. Skerlos, Costs to achieve target net emissions reductions in the US electric sector using direct air capture, *Environ. Res. Lett.*, 2019, **14**, 084013.
- 3 O. Edenhofer, Climate Change. Contribution of Working Group III to the Fifth Assessment Report of the Intergovernmental Panel on Climate Change, *Technical Report*, 2014.
- 4 GCCSI. Global status report of CCS: 2022. [https://status22.globalccsinstitute.com/\(2022\)](https://status22.globalccsinstitute.com/(2022)).
- 5 P. S. Ringrose and T. A. Meckel, Maturing global CO<sub>2</sub> storage resources on offshore continental margins to achieve 2DS emissions reductions, *Sci. Rep.*, 2019, 1–10.
- 6 E. Abramson, D. McFarlane and J. Brown, Transport Infrastructure for Carbon Capture and Storage, Whitepaper on Regional Infrastructure for Midcentury Decarbonization, 2020, [https://www.betterenergy.org/wp-content/uploads/2020/06/GPI\\_RegionalCO2Whitepaper.pdf](https://www.betterenergy.org/wp-content/uploads/2020/06/GPI_RegionalCO2Whitepaper.pdf).
- 7 IEA, CCUS around the world, <https://www.iea.org/reports/ccus-around-the-world> (2021).
- 8 S. E. Baker, *et al.*, Getting to Neutral: Options for Negative Carbon Emissions in California, <http://www.osti.gov/servlets/purl/1597217/> (2019), DOI: [10.2172/1597217](https://doi.org/10.2172/1597217).
- 9 M. Aresta, *Carbon dioxide recovery and utilization*, Springer Science & Business Media, 2013.
- 10 S. M. Jarvis and S. Samsatli, Technologies and infrastructures underpinning future CO<sub>2</sub> value chains: A comprehensive review and comparative analysis, *Renewable Sustainable Energy Rev.*, 2018, **85**, 46–68.
- 11 T. Lim, B. R. Ellis and S. J. Skerlos, Mitigating CO<sub>2</sub> emissions of concrete manufacturing through CO<sub>2</sub>-enabled binder reduction, *Environ. Res. Lett.*, 2019, **14**, 114014.



- 12 Board, Ocean Studies, and National Academies of Sciences, Engineering, and Medicine, Negative emissions technologies and reliable sequestration: A research agenda, 2019, DOI: [10.17226/25259](https://doi.org/10.17226/25259).
- 13 L. A. Bullock, A. Yang and R. C. Darton, Kinetics-informed global assessment of mine tailings for CO<sub>2</sub> removal, *Sci. Total Environ.*, 2022, **808**, 152111.
- 14 B. C. O'Neill, *et al.*, A new scenario framework for climate change research: The concept of shared socioeconomic pathways, *Clim. Change*, 2014, **122**, 387–400.
- 15 J. Rogelj, *et al.*, Scenarios towards limiting global mean temperature increase below 1.5 °C, *Nat. Clim. Change*, 2018, **8**(8), 325–332.
- 16 IEA. CO<sub>2</sub> Capture and Utilisation, <https://www.iea.org/reports/co2-capture-and-utilisation> (2022).
- 17 M. Ozaki and T. Ohsumi, CCS from multiple sources to offshore storage site complex via ship transport, *Energy Procedia*, 2011, **4**, 2992–2999.
- 18 B. Y. Yoo, S. G. Lee, K. P. Rhee, H. S. Na and J. M. Park, New CCS system integration with CO<sub>2</sub> carrier and liquefaction process, *Energy Procedia*, 2011, **4**, 2308–2314.
- 19 T. Barrett, DNV awards KNCC AiP for high pressure LCO<sub>2</sub> transport concept, (2022).
- 20 D. W. Keith, G. Holmes, D. St. Angelo and K. Heidel, A Process for Capturing CO<sub>2</sub> from the Atmosphere, *Joule*, 2018, **2**, 1573–1594.
- 21 S. Fuss, *et al.*, Negative emissions—Part 2: Costs, potentials and side effects, *Environ. Res. Lett.*, 2018, **13**, 063002.
- 22 S. Jackson and E. Brodal, A comparison of the energy consumption for CO<sub>2</sub> compression process alternatives, *IOP Conf. Ser.: Earth Environ. Sci.*, 2018, **167**, 012031.
- 23 E. De Lena, *et al.*, Techno-economic analysis of calcium looping processes for low CO<sub>2</sub> emission cement plants, *Int. J. Greenhouse Gas Control*, 2019, **82**, 244–260.
- 24 M. P. S. Santos, V. Manovic and D. P. Hanak, Unlocking the potential of pulp and paper industry to achieve carbon-negative emissions via calcium looping retrofit, *J. Cleaner Prod.*, 2021, **280**, 124431.
- 25 Y. Sun, *et al.*, Decarbonising the iron and steel sector for a 2 °C target using inherent waste streams, *Nat. Commun.*, 2022, **13**(13), 1–8.
- 26 N. McQueen, P. Kelemen, G. Dipple, P. Renforth and J. Wilcox, Ambient weathering of magnesium oxide for CO<sub>2</sub> removal from air, *Nat. Commun.*, 2020, **11**(11), 1–10.
- 27 K. Sumida, *et al.*, Carbon dioxide capture in metal–organic frameworks, *Chem. Rev.*, 2011, **112**, 724–781.
- 28 R. Veneman, W. Zhao, Z. Li, N. Cai and D. W. F. Brilman, Adsorption of CO<sub>2</sub> and H<sub>2</sub>O on supported amine sorbents, *Energy Procedia*, 2014, **63**, 2336–2345.
- 29 E. Southall and L. Lukashuk, Potential Deployment and Integration of Liquid Organic Hydrogen Carrier Technology within Different Industries: Liquid organic hydrogen carrier technology to support on demand hydrogen supply and energy storage, *Johnson Matthey Technol. Rev.*, 2022, **66**, 259–270.
- 30 A. Anastasopoulou, Technoeconomic Analysis of Metal–Organic Frameworks for Bulk Hydrogen Transportation, *Energy Environ. Sci.*, 2021, **14**, 1083–1094.
- 31 J. Galos, M. Sutcliffe, D. Cebon, M. Piecyk and P. Greening, Reducing the energy consumption of heavy goods vehicles through the application of lightweight trailers: Fleet case studies, *Transp. Res. Part D Transp. Environ.*, 2015, **41**, 40–49.
- 32 E. W. Lemmon, I. H. Bell, M. L. Huber and M. O. McLinden, Thermophysical Properties of Fluid Systems. in *Hemistry WebBook, NIST Standard Reference Database Number 69*, ed. P. J. Linstrom and W. G. Mallard, 2022.
- 33 CO<sub>2</sub> pipeline infrastructure, [www.globalccsinstitute.com/archive/hub/publications/120301/CO2-pipeline-infrastructure.pdf](http://www.globalccsinstitute.com/archive/hub/publications/120301/CO2-pipeline-infrastructure.pdf) (2013).
- 34 S. P. Peletiri, N. Rahmanian and I. M. Mujtaba, CO<sub>2</sub> Pipeline Design: A Review, *Energies*, 2018, **11**, 2184.
- 35 V. E. Onyebuchi, A. Kolios, D. P. Hanak, C. Biliyok and V. Manovic, A systematic review of key challenges of CO<sub>2</sub> transport via pipelines, *Renewable Sustainable Energy Rev.*, 2018, **81**, 2563–2583.
- 36 G. Heddle, H. Herzog and M. Klett, *The economics of CO<sub>2</sub> storage*, 2003.
- 37 S. Deutz and A. Bardow, Life-cycle assessment of an industrial direct air capture process based on temperature–vacuum swing adsorption, *Nat. Energy*, 2021, **6**(6), 203–213.
- 38 B. Omell and D. Bhattacharyya, Carbon Capture Simulation Initiative (CCSI) Compressor User Manual, 2018.
- 39 Inventory of U.S. Greenhouse Gas Emissions and Sinks: Tables A-32, A-38, and A-232, [www.eia.gov/environment/emissions/CO2\\_vol\\_mass.php](http://www.eia.gov/environment/emissions/CO2_vol_mass.php).
- 40 EIA-923 emissions survey data, [www.eia.gov/tools/faqs/faq.php?id=74&t=11](http://www.eia.gov/tools/faqs/faq.php?id=74&t=11) (2021).
- 41 H. Furukawa, *et al.*, Ultrahigh porosity in metal-organic frameworks, *Science*, 2010, **329**, 424–428.
- 42 S. Himeno, T. Komatsu and S. Fujita, High-Pressure Adsorption Equilibria of Methane and Carbon Dioxide on Several Activated Carbons, *J. Chem. Eng. Data*, 2005, **50**, 369–376.
- 43 H. G. T. Nguyen, *et al.*, A reference high-pressure CO<sub>2</sub> adsorption isotherm for ammonium ZSM-5 zeolite: results of an interlaboratory study, *Adsorption*, 2018, **24**, 531–539.
- 44 Y. Wang and M. D. LeVan, Adsorption Equilibrium of Carbon Dioxide and Water Vapor on Zeolites 5A and 13X and Silica Gel: Pure Components, *J. Chem. Eng. Data*, 2009, **54**, 2839–2844.
- 45 S. M. Amorim, M. D. Domenico, T. L. P. Dantas, H. J. José and R. F. P. M. Moreira, Lithium orthosilicate for CO<sub>2</sub> capture with high regeneration capacity: Kinetic study and modeling of carbonation and decarbonation reactions, *Chem. Eng. J.*, 2016, **283**, 388–396.
- 46 J. Zhang, R. Singh and P. A. Webley, Alkali and alkaline-earth cation exchanged chabazite zeolites for adsorption based CO<sub>2</sub> capture, *Microporous Mesoporous Mater.*, 2008, **111**, 478–487.
- 47 C. F. Martín, *et al.*, On the limits of CO<sub>2</sub> capture capacity of carbons, *Sep. Purif. Technol.*, 2010, **74**, 225–229.



- 48 C. W. Kamienski, D. P. McDonald, M. W. Stark and J. R. Papcun, Lithium and lithium compounds, *Kirk-Othmer Encyclopedia of Chemical Technology*, 2000.
- 49 H. M. Baek, Possibility of military service-regeneration of LiOH for submarines and improvement in CO<sub>2</sub> scrubbing performance of LiOH canisters, *J. Adv. Mar. Eng. Technol.*, 2022, **46**, 115–121.
- 50 F. Meng, J. McNeice, S. S. Zadeh and A. Ghahreman, Review of Lithium Production and Recovery from Minerals, Brines, and Lithium-Ion Batteries, *Miner. Process. Extr. Metall. Rev.*, 2021, **42**, 123–141.
- 51 A. Gambhir and M. Tavoni, Direct Air Carbon Capture and Sequestration: How It Works and How It Could Contribute to Climate-Change Mitigation, *One Earth*, 2019, **1**, 405–409.
- 52 M. Mahmoudkhani and D. W. Keith, Low-energy sodium hydroxide recovery for CO<sub>2</sub> capture from atmospheric air-Thermodynamic analysis, *Int. J. Greenhouse Gas Control*, 2009, **3**, 376–384.
- 53 C. Thieme, Sodium Carbonates, *Ullmann's Encyclopedia of Industrial Chemistry*, 2000, DOI: [10.1002/14356007.A24\\_299](https://doi.org/10.1002/14356007.A24_299).
- 54 H. Schultz, G. Bauer, E. Schachl, F. Hagedorn and P. Schmittinger, Potassium Compounds, *Ullmann's Encyclopedia of Industrial Chemistry*, 2000, DOI: [10.1002/14356007.A22\\_039](https://doi.org/10.1002/14356007.A22_039).
- 55 V. Vágvölgyi, *et al.*, Conventional and controlled rate thermal analysis of nesquehonite Mg(HCO<sub>3</sub>)(OH)·2(H<sub>2</sub>O), *J. Therm. Anal. Calorim.*, 2008, **942**(94), 523–528.
- 56 R. C. Ropp, Group 14 (C, Si, Ge, Sn, and Pb) Alkaline Earth Compounds, *Encycl. Alkaline Earth Compd.*, 2013, 351–480, DOI: [10.1016/B978-0-444-59550-8.00005-3](https://doi.org/10.1016/B978-0-444-59550-8.00005-3).
- 57 R. C. Ropp, Group 16 (O, S, Se, Te) Alkaline Earth Compounds, *Encycl. Alkaline Earth Compd.*, 2013, 105–197, DOI: [10.1016/B978-0-444-59550-8.00003-X](https://doi.org/10.1016/B978-0-444-59550-8.00003-X).
- 58 A. H. Ruhaimi, M. A. A. Aziz and A. A. Jalil, Magnesium oxide-based adsorbents for carbon dioxide capture: Current progress and future opportunities, *J. CO<sub>2</sub> Util.*, 2021, **43**, 101357, DOI: [10.1016/j.jcou.2020.101357](https://doi.org/10.1016/j.jcou.2020.101357).
- 59 J. D. Rodriguez-Blanco, S. Shaw, P. Bots, T. Roncal-Herrero and L. G. Benning, The role of Mg in the crystallization of monohydrocalcite, *Geochim. Cosmochim. Acta*, 2014, **127**, 204–220.
- 60 J. M. Huggett, B. P. Schultz, D. J. Shearman and A. J. Smith, The petrology of ikaite pseudomorphs and their diagenesis, *Proc. Geol. Assoc.*, 2005, **116**, 207–220.
- 61 G. S. Kumar, A. Ramakrishnan and Y.-T. Hung, Lime Calcination, *Adv. Physicochem. Treat. Technol.*, 2007, 611–633, DOI: [10.1007/978-1-59745-173-4\\_14](https://doi.org/10.1007/978-1-59745-173-4_14).
- 62 M. Bilton, A. P. Brown and S. J. Milne, Investigating the optimum conditions for the formation of calcium oxide, used for CO<sub>2</sub> sequestration, by thermal decomposition of calcium acetate, *J. Phys. Conf. Ser.*, 2012, **371**, 012075.
- 63 ICSC 0707 - Oxalic Acid Dihydrate.
- 64 M. König, S. H. Lin, J. Vaes, D. Pant and E. Klemm, Integration of aprotic CO<sub>2</sub> reduction to oxalate at a Pb catalyst into a GDE flow cell configuration, *Faraday Discuss.*, 2021, **230**, 360–374.
- 65 E. Schuler, M. Demetriou, N. R. Shiju and G. J. M. Gruter, Towards Sustainable Oxalic Acid from CO<sub>2</sub> and Biomass, *ChemSusChem*, 2021, **14**, 3636–3664.
- 66 G. Lapidus, D. Barton and P. E. Yankwich, Kinetics and stoichiometry of the gas-phase decomposition of oxalic acid, *J. Phys. Chem.*, 1964, **68**, 1863–1865.
- 67 K. Tedsree, *et al.*, Hydrogen production from formic acid decomposition at room temperature using a Ag-Pd core-shell nanocatalyst, *Nat. Nanotechnol.*, 2011, **6**, 302–307.
- 68 S. Kar, A. Goeppert and G. K. S. Prakash, Combined CO<sub>2</sub> Capture and Hydrogenation to Methanol: Amine Immobilization Enables Easy Recycling of Active Elements, *ChemSusChem*, 2019, **12**, 3172–3177.
- 69 E. Alberico and M. Nielsen, Towards a methanol economy based on homogeneous catalysis: methanol to H<sub>2</sub> and CO<sub>2</sub> to methanol, *Chem. Commun.*, 2015, **51**, 6714–6725.
- 70 R. Andika, *et al.*, Co-electrolysis for power-to-methanol applications, *Renewable Sustainable Energy Rev.*, 2018, **95**, 227–241.
- 71 Carbon dioxide-to-methanol catalyst ignites 'fuel from air' debate | Research | Chemistry World, <https://www.chemistryworld.com/news/carbon-dioxide-to-methanol-catalyst-ignites-fuel-from-air-debate/9339.article>.
- 72 S. Zhang, X. Jing, Y. Wang and F. Li, Towards Carbon-Neutral Methanol Production from Carbon Dioxide Electro-reduction, *ChemNanoMat*, 2021, **7**, 728–736.
- 73 S. Bhardwaj, A. Biswas, M. Das and R. S. Dey, Nanostructured Cu foam and its derivatives: emerging materials for the heterogeneous conversion of CO<sub>2</sub> to fuels, *Sustainable Energy Fuels*, 2021, **5**, 2393–2414.
- 74 G. Garcia, E. Arriola, W. H. Chen and M. D. De Luna, A comprehensive review of hydrogen production from methanol thermochemical conversion for sustainability, *Energy*, 2021, **217**, 119384.
- 75 A. M. Ranjekar and G. D. Yadav, Steam Reforming of Methanol for Hydrogen Production: A Critical Analysis of Catalysis, Processes, and Scope, *Ind. Eng. Chem. Res.*, 2021, **60**, 89–113.
- 76 B. S. Crandall, T. Brix, R. S. Weber and F. Jiao, Techno-Economic Assessment of Green H<sub>2</sub>Carrier Supply Chains, *Energy Fuels*, 2022, **37**, 1441–1450, DOI: [10.1021/acs.energyfuels.2c03616](https://doi.org/10.1021/acs.energyfuels.2c03616).
- 77 Y. K. A. Migdadi, A. A. Khalifa, A. Al-Swidi, A. I. Amhamed and M. H. El-Naas, A Conceptual Framework of Customer Value Proposition of CCU-Formic Acid Product, *Sustainability*, 2022, **14**, 16351, DOI: [10.3390/su142416351](https://doi.org/10.3390/su142416351).
- 78 B. Zaidman, H. Wiener and Y. Sasson, Formate salts as chemical carriers in hydrogen storage and transportation, *Int. J. Hydrogen Energy*, 1986, **11**, 341–347.
- 79 S. Chatterjee, I. Dutta, Y. Lum, Z. Lai and K. W. Huang, Enabling storage and utilization of low-carbon electricity: power to formic acid, *Energy Environ. Sci.*, 2021, **14**, 1194–1246.
- 80 P. Duarah, D. Haldar, V. S. K. Yadav and M. K. Purkait, Progress in the electrochemical reduction of CO<sub>2</sub> to formic acid: A review on current trends and future prospects, *J. Environ. Chem. Eng.*, 2021, **9**, 106394.





- 81 D. Wei, R. Sang, P. Sponholz, H. Junge and M. Beller, Reversible hydrogenation of carbon dioxide to formic acid using a Mn-pincer complex in the presence of lysine, *Nat. Energy*, 2022, **75**(7), 438–447.
- 82 W. B. Li and C. Yu, *et al.*, Recent advances in the electro-reduction of carbon dioxide to formic acid over carbon-based materials, *New Carbon Mater.*, 2022, **37**, 277–289.
- 83 L. Fan, C. Xia, P. Zhu, Y. Lu and H. Wang, Electrochemical CO<sub>2</sub> reduction to high-concentration pure formic acid solutions in an all-solid-state reactor, *Nat. Commun.*, 2020, **11**(11), 1–9.
- 84 Z. Sun, T. Ma, H. Tao, Q. Fan and B. Han, Fundamentals and Challenges of Electrochemical CO<sub>2</sub> Reduction Using Two-Dimensional Materials, *Chem*, 2017, **3**, 560–587.
- 85 P.-L. Ragon and F. Rodríguez, CO<sub>2</sub> emissions from trucks in the EU: An analysis of the heavy-duty CO<sub>2</sub> standards baseline data, <https://trid.trb.org/view/1893383> (2021).
- 86 N. Amghar, *et al.*, The SrCO<sub>3</sub>/SrO system for thermochemical energy storage at ultra-high temperature, *Sol. Energy Mater. Sol. Cells*, 2022, **238**, 111632.
- 87 S. T. McCoy and E. S. Rubin, An engineering-economic model of pipeline transport of CO<sub>2</sub> with application to carbon capture and storage, *Int. J. Greenhouse Gas Control*, 2008, **2**, 219–229.
- 88 F. Chen and T. Morosuk, Exergetic and Economic Evaluation of CO<sub>2</sub> Liquefaction Processes, *Energies*, 2021, **14**, 7174, DOI: [10.3390/en14217174](https://doi.org/10.3390/en14217174).
- 89 N. Dawass, *et al.*, Solubilities and Transport Properties of CO<sub>2</sub>, Oxalic Acid, and Formic Acid in Mixed Solvents Composed of Deep Eutectic Solvents, Methanol, and Propylene Carbonate, *J. Phys. Chem. B*, 2022, 3572–3584.
- 90 O. Gutiérrez-Sánchez, *et al.*, Electrochemical Conversion of CO<sub>2</sub> from Direct Air Capture Solutions, *Energy Fuels*, 2022, **21**, 13115–13123.
- 91 M. Aresta, A. Dibenedetto and A. Angelini, Catalysis for the valorization of exhaust carbon: from CO<sub>2</sub> to chemicals, materials, and fuels. Technological use of CO<sub>2</sub>, *Chem. Rev.*, 2014, **114**, 1709–1742.
- 92 R. Singh, M. Singh and S. Gautam, Hydrogen economy, energy, and liquid organic carriers for its mobility, *Mater. Today Proc.*, 2021, **46**, 5420–5427.
- 93 Q. Song, *et al.*, A comparative study on energy efficiency of the maritime supply chains for liquefied hydrogen, ammonia, methanol and natural gas, *Carbon Capture Sci. Technol.*, 2022, **4**, 100056.
- 94 D. DeSantis, *et al.*, Techno-economic analysis of metal-organic frameworks for hydrogen and natural gas storage, *Energy Fuels*, 2017, **31**, 2024–2032.

